AD_____

Award Number: W81XWH-06-1-0417

TITLE: Immunology, Systems Biology, and Immunotherapy of Breast Cancer

PRINCIPAL INVESTIGATOR: Peter P. Lee, M.D.

CONTRACTING ORGANIZATION: Stanford University
Stanford, CA 94305

REPORT DATE: March 2008

TYPE OF REPORT: Annual

PREPARED FOR: U.S. Army Medical Research and Materiel Command
Fort Detrick, Maryland 21702-5012

DISTRIBUTION STATEMENT: Approved for Public Release;
Distribution Unlimited

REPORT DOCUMENTATION PAGE

Form Approved
OMB No. 0704-0188

1. REPORT DATE	2. REPORT TYPE	3. DATES COVERED
31-03-2008	Annual	1 MAR 2007 - 28 FEB 2008

4. TITLE AND SUBTITLE
Immunology, Systems Biology, and Immunotherapy of Breast Cancer

5a. CONTRACT NUMBER

5b. GRANT NUMBER
W81XWH-06-1-0417

5c. PROGRAM ELEMENT NUMBER

6. AUTHOR(S)
Peter P. Lee, M.D.

Email: ppl@stanford.edu

5d. PROJECT NUMBER

5e. TASK NUMBER

5f. WORK UNIT NUMBER

7. PERFORMING ORGANIZATION NAME(S) AND ADDRESS(ES)

Stanford University
Stanford, CA 94305

8. PERFORMING ORGANIZATION REPORT NUMBER

9. SPONSORING / MONITORING AGENCY NAME(S) AND ADDRESS(ES)
U.S. Army Medical Research and Materiel Command
Fort Detrick, Maryland 21702-5012

10. SPONSOR/MONITOR'S ACRONYM(S)

11. SPONSOR/MONITOR'S REPORT NUMBER(S)

12. DISTRIBUTION / AVAILABILITY STATEMENT
Approved for Public Release; Distribution Unlimited

13. SUPPLEMENTARY NOTES

14. ABSTRACT

In year 2, we made substantial progress in multiple areas. We have an efficient system in place to recruit patients into this study and procure their samples. However, limited numbers of subjects available and limited amounts of clinical materials available from each subject remain major challenges to the success of this project – we continually attempt to address and solve this issue. We have developed a powerful set of immunological assays and molecular tools to study these samples in greater detail than previously possible. We are constantly striving to minimize the numbers of cells we need to generate useful data, and have to make decisions to pursue only the most promising assays with many samples. We are beginning to uncover dramatic changes in the immune cell populations within tumors, TDLNs, and peripheral blood from breast cancer patients. These will provide important insights into how breast cancer alters the host immune system. We look forward in the coming year to build upon the early data we are generating to come up with meaningful observations and insights into the immunobiology of breast cancer. In the coming year and beyond, we will also begin to make progress on the systems biology that will ultimately position us for the immunotherapy of breast cancer.

15. SUBJECT TERMS
Breast cancer, immunology, immunotherapy, systems biology

16. SECURITY CLASSIFICATION OF:			17. LIMITATION OF ABSTRACT	18. NUMBER OF PAGES	19a. NAME OF RESPONSIBLE PERSON
a. REPORT	b. ABSTRACT	c. THIS PAGE			USAMRMC
U	U	U	UU	37	19b. TELEPHONE NUMBER *(include area code)*

Annual Progress Report 3/1/07-2/29/08
DoD Era of Hope Scholar Award
Immunology, Systems Biology, and Immunotherapy of Breast Cancer
Peter P. Lee, M.D.
Stanford University

INTRODUCTION

Breast cancer patients with similar tumor characteristics may have vastly different clinical courses, response to therapy, and outcome. Several lines of evidence now suggest that the host immune response may play a significant role in modulating disease progression in cancer. A complex interplay exists between the host immune response and tumor cells as a critical determinant in clinical outcome. These factors remain poorly understood. By comprehensively studying the dynamics between breast cancer and the immune response using an integrative systems approach, we hope to uncover opportunities for vastly different immunotherapy approaches than what are available today. We seek to move beyond the current paradigm of eliciting immune responses against defined antigens via vaccination, as this strategy alone does not appear to be effective in a number of clinical trials for melanoma and other cancers. Rather, we seek strategies that specifically modulate tumor-immune cell interactions and block cancer-induced immune dysfunction on a systemic and local level (at tumor sites and draining lymph nodes). In this project, we use a number of novel immunological approaches to look for evidence of immune cell dysfunction within the tumor or tumor-draining lymph nodes (TDLNs) from breast cancer patients. This includes archived samples from patients with at least five year survival data, and fresh samples from newly diagnosed patients. We use DNA microarrays to analyze the gene expression patterns of purified tumor and immune cells, focusing on gene networks and cross-talk between tumor and immune cells. We generate high-resolution images of tumor and TDLN sections and develop image analysis algorithms to assess the spatial arrangement and grouping of tumor and immune cells with respect to each other that may have biological significance. Using statistics and mathematical tools, we will integrate the complex data generated from all of these studies and correlate them with clinical parameters. Lastly, our observations will be combined into a mathematical model that will enable us to perform *in silico* experiments to quickly test novel therapeutic strategies for breast cancer. This work may lead to novel diagnostic tools to help predict clinical outcome and guide therapy in breast cancer patients. We also hope to find new insights into the mechanisms of immune evasion by breast cancer cells and ultimately new treatment strategies for breast cancer directed specifically at altering the biology of TDLNs.

BODY

After the first year of intense infrastructure building, the second year of this award yielded early progress in multiple areas of this project that will be described in more detail below. Our team currently consists of two excellent research associates, two PhD postdoctoral fellows, and one graduate student. This represents the full complement of personnel that can be supported by this award. As will become clear, vast amounts of data are being generated in this project. A third PhD postdoctoral fellow with expertise in bioinformatics, data integration and analysis would greatly enhance the overall project and help us to achieve faster and more

results. We work closely with our surgery and pathology colleagues to identify, recruit, and consent subjects, and to obtain samples from the operating room to pathology and eventually to my laboratory. We continue to refine our protocols to maximize recovery of immune cells from tumor and lymph node specimens, and to optimize methods for analysis of fresh and archive samples by flow cytometry, immunohistology, immunoflourescence, function assays, and DNA microarray analysis. Below is a summary of our progress in relation to my proposed SOW.

Experiment Strategy
To fully understand tumor-immune cell interactions in breast cancer, our strategy is to compare the immune cells and tumor cells within three distinct compartments: the tumor, tumor-draining lymph nodes (TDLNs), and blood. We approach this at both the molecular and cellular levels. At the molecular level, gene expression profiling of immune cells and tumor cells within the tumor site and TDLNs are being carried out. At the cellular level, immunologic functions of immune cells are being studied and compared across these three compartments.

A. Immunological Analyses

Originally proposed in the SOW:
1. Analysis of archived samples of tumor and TDLN from breast cancer patients with at least 5 years of clinical follow-up data. Tumor and immune cell markers will be identified via immunohistochemical (IHC) staining and in-situ hybridization (ISH). Images will be acquired in high resolution using an automated imaging system (BLISS), and data will be acquired using automated software. Over 50 immune and tumor markers will be assessed. To facilitate these complex studies, we will also explore the use of tissue microarrays (TMA). This would enable us to analyze sections from 100-400 samples on each slide. We will first perform a pilot study to ensure that the TMA method is compatible for our studies and would not be negatively impacted by the architectural heterogeneity within TDLN. (months 0-60)
2. Analysis of live cells from fresh tumor, TDLN, blood, and possibly bone marrow from newly diagnosed or relapsed breast cancer patients undergoing surgery or treatment. Assays include flow cytometry (up to 12 colors), peptide-MHC tetramer analysis, sorting, functional responses (e.g. cytotoxicity, cytokine release, anergy, apoptosis, proliferation), and others. (months 6-60)
3. Generation of T cell lines and tumor cell lines from fresh tumor and TDLN samples for further detailed analyses. (months 6-60)
4. If the above studies demonstrate immune cell dysfunction within tumor or TDLN, but by themselves do not reveal any definitive mechanisms, then we will undertake in vivo studies with mouse models of de novo breast cancer to address the early events in immune dysfunction. (months 24-60)

Sample Acquisition
At the end of year 2, a total of 93 breast cancer patients have been enrolled into this study. All subjects were newly diagnosed without a history of any immune disorder prior to breast cancer diagnosis and had their surgical treatments at Stanford University Medical Center.

Written informed consent has been obtained from all participants according to Stanford IRB, DoD HSRRB, and HIPAA regulations. Patients' heparinized peripheral blood samples, breast tumor tissue, tumor draining lymph node (TDLN: non-sentinel lymph node and/or sentinel lymph node aspirates) have been collected for this study. Clinical data (stage, grade, ER/PR/Her-2/neu status) for each participant has been recorded without patient identifying information.

Sample Processing

1. Pilot study

Since we seek to compare gene expression profiles of cells across three anatomic compartments, which require different sample processing procedures, it is important to minimize influences from different sample processing protocols, particularly the conditions we use to process the breast tissue. Therefore a pilot study using several healthy donor PBMCs was performed to determine the potential influence of various sample processing procedures (Ficoll-Hypaque density gradient centrifugation, red blood cell lysis treatment, cryopreservation, dissociation enzyme digestion, and overnight culture) on gene expression. Immune cells were processed accordingly and quantitative real-time PCR (qPCR) was used to check for gene expression changes of housekeeping genes. Two housekeeping genes (GAPDH and YWHAZ), which are stably expressed in immune cells, were used for this purpose. In addition, changes of cell surface marker expression, proliferation capability and cytokine profile were determined. A sample processing procedure with minimal influences on gene expression, cell surface marker expression, cell proliferation capability and cytokine profile was selected.

2. Peripheral blood immune cell isolation

Immune cells from peripheral blood are separated by Ficoll-Hypague density gradient centrifugation. RBC lysis buffer treatment is used to remove residual red blood cells and to ensure an accurate counting using hemocytometer. A total of 1 million isolated immune cells are preserved in Trizol (Invitrogen) for RNA isolation and the remaining cells are cryopreserved in liquid nitrogen until further use.

3. Breast Tissue dissociation and immune cell/tumor cell isolation

Immediately after surgery, breast tumor tissues are minced and dissociated with type III collagenase and DNase I for 1-2 hour to generate single cell suspensions. The cells are then stained with cell surface marker listed in Table 1. The two major cell populations in breasts tumor tissue - immune cells ($CD45^+ESA^-CD140\beta^-$), epithelial/tumor cells ($ESA^+CD45^-CD140\beta^-$) - are purified via FACS sorting. Up to 1 million sorted immune cells or tumor cells are preserved in Trizol for RNA isolation and the remaining cells are cryopreserved in liquid nitrogen until further use. To ensure the breast tissue specimen does indeed contain tumor cells, the tumor tissue is bisected, and submitted for histological processing using hematoxylin and eosin staining, and examined by a pathologist specializing in cytology.

4. TDLNs

Immediately after lymph node dissection, fine-needle aspirates of sentinel lymph nodes are collected. For non-sentinel lymph nodes, half of each node is excised and minced to generate single cell suspensions. For grossly tumor involved lymph nodes, the minced specimen is

subjected to enzymatic dissociation with type III collagenase and DNase I. A multicolor flow cytometry panel is used to stain cells from TDLNs. Immune cells and/or tumor cells are purified through FACS sorting. Up to 1 million isolated immune cells or tumor cells are preserved in Trizol for RNA isolation and the remaining cells are cryopreserved in liquid nitrogen until further use.

Table 1. Four Color Flow Cytometry Panel for Sorting

Cells/Subsets of Interest	Surace marker
epithelial/tumor cells	epithelial specific antigen (ESA)
fibroblast cells	CD140β
immune cells (lymphocytes/monocytes/granulocytes)	CD45
dead cell exclusion marker	ViVID

Flow cytometry-based functional assays of lymphocytes

To assess the basic immunologic functions of human lymphocytes, we proposed to develop flow cytometry-based functional assays to measure proliferative responses and Th1/Th2 cytokine production of lymphocytes.

Cytokine profile

Freshly isolated immune cells were stimulated with phorbol esters/Ionomycin for 20 hour and protein transport inhibitor monensin was added to accumulate cytokine in the Golgi complex to enhance the detections of cytokine producing cells. The surface markers used for phenotype characterization include ESA-FITC, CD45-PE Cy7, CD19-APC, CD3-PerCP, CD8-PE AF700 and dead cell exclusion marker ViVID. The intracellular cytokine expression and phenotype characterization of cells were analyzed on a FACSAria (BD). Isolated immune cells from tumor free lymph nodes (n=18), tumor involving lymph nodes (n=5) and peripheral blood (n=2) were evaluated for their ability to produce type 1 cytokine (IL-2, IFNγ) and type 2 cytokine (IL-4, IL-10, TGFβ). The majority of cytokines synthesized by $CD8^+$ T cells, $CD4^+$ T cells and B cells is classified as type 1 cytokines, i.e. IL-2, IFNγ. Type 2 cytokine (IL4/IL10/TGFβ) was not detectable (<1% positive in all cases). Although the sample size is small, there is no significant difference in the cytokine biosynthesis between tumor free/tumor involved nodes and peripheral blood. No significant difference is observed in different stages of the disease. To evaluate the influence of tumor cells on cytokine production, the cytokine profiles of immune cells for tumor involving nodes were also studied before and after depletion of the tumor cells. There is no difference observed. Thus far the information obtained through intracellular cytokine staining is limited to IL-2, IFNγ. Therefore we decide to employ a different strategy to investigate the cytokine profiles, which can be combined with the CFSE-based proliferation assay.

CFSE-based proliferation assay

A 9 color, 11 parameter flow cytometry panel was developed for the CFSE-based proliferation assay. In brief, freshly isolated immune cells were labeled with CFSE followed by stimulation with phorbol esters/Ionomycin for 115hour. The supernatant of the cultured cells was collected and stored at -80°C for multiplex analysis of the cytokines produced during culture. The stimulated/unstimulated cells were stained with CD45-PE Cy7, CD19-PE

TR, CD3-AF700, CD8-APC Cy7, CD86 PE AF700, ViVID and analyzed on a FACSAria (BD). So far we have analyzed a total of 25 patient samples, which include immune cells from 16 tumor free lymph nodes, 7 tumor involving lymph nodes and 2 peripheral blood samples. Apart from these, we also analyzed 5 control peripheral blood samples from healthy donors. It seems that lymphocytes from lymph nodes (regardless of tumor involvement) have less capability to proliferate compared with lymphocytes from peripheral blood (Figure A1). Studies with mice showed similar lymphocytes proliferation capability between lymph node and blood (Data not shown), suggesting a decreased proliferating capability of lymphocytes in breast cancer lymph nodes. Paired peripheral blood lymphocytes for these lymph node samples were cryopreserved and will be analyzed in a batch to increase the sample size and allow comparison of proliferation capability of lymphocytes in the same individual.

It has been shown that B cells in the lymph nodes are potent antigen presenting cells and antigen presentation by resting B cells can induce T cell tolerance *in vivo* (Rodríguez-Pinto D. et al, 2005). Therefore we included CD86 in this assay to study the antigen presentation function of B cells. The expressions of CD86 on B cells are significantly decreased in breast cancer patients (peripheral blood, tumor free lymph nodes, tumor involving lymph nodes) compared with control peripheral blood ($p=0.0046$). Upon activation, the upregulation of CD86 expressions are similar between patients and controls (Data not shown).

Interferon Signaling Defect in Lymphocytes from Breast Cancer Patients

We recently demonstrated that IFN signaling is impaired in peripheral blood lymphocytes from melanoma patients (Critchely-Thorne, *et al*). To determine whether a similar immune defect arises in breast cancer patients, we assessed the functional response of peripheral blood lymphocytes from breast cancer patients (as compared to age-matched healthy controls) by phosflow analysis (detection of STAT1-pY701) upon stimulation with IFN-α and IFN-γ. In addition, we included different subsets of cells, such as T regs, NK cells, and naïve, effector, memory T cells. Data was analyzed using Wilcoxon-Mann-Whitney test (95% CI) in a statistical application, R, to calculate the exact p-values for each of the comparisons. P-values of < 0.05 were considered significant.

Our healthy controls were composed of both males and females, so we first determined whether samples from different sexes were statistically different from each other before we compared the complete healthy population to breast cancer patients (all female). We found that fold induction of STAT1-pY701 was not statistically different between male and female healthy controls for both IFN-α and IFN-γ stimulation (Figure A2 and A3, respectively), and therefore, we included all healthy patients in our analysis.

Fold induction of STAT1-pY701 was significantly reduced in breast cancer patients compared to healthy controls in response to IFN-α stimulation in lymphocytes, T cells, B cells, NK cells, and T reg cells (Figure A4). In contrast, the fold induction of STAT1-pY701 in response to IFN-γ stimulation in T cells, NK cells, and T reg cells was not significant. However, IFN-γ stimulation of B cells showed a profound reduction of STAT1-pY701 (Figure A5). The lymphocyte population for IFN-γ stimulation in Figure A5a shows a

significant decrease in the fold induction of STAT1-pY701, however, this is most likely a reflection of the reduction of STAT1-pY701 of B cells.

To determine if the reduced fold induction of STAT1-pY701 may be classified by breast cancer stage, we separated the breast cancer patients by stage. The reduced fold change in STAT1-pY701 in response to IFN-α or –γ was equally observed in stages II, III and IV breast cancer patients for lymphocytes, T cells, B cells, NK cells, and/or Treg cells (Figure A6 and Figure A7, respectively). Interestingly, the reduced fold change in IFN-γ-stimulated B cells was quite significant in all stages of breast cancer. P-values were not generated for both IFN-α and IFN-γ-stimulated T reg cells for stage II and stage IV due to small sample size.

Some of the breast cancer patients analyzed had received neo-adjuvant or adjuvant therapy when blood was obtained. We determined whether the reduced fold induction of STAT1-pY701 was a consequence of therapy. We compared breast cancer patients who had received therapy to those who did not receive therapy for both Type I and Type II IFN stimuli (Figure 7 and 8, respectively). Generating p-values > 0.05 for all cell subsets demonstrated no significant difference between patients who received neo-adjuvant or adjuvant therapy compared to patients who did not undergo therapy.

- We have demonstrated there is a defect of IFN signaling in breast cancer patients' peripheral blood leukocytes, regardless of therapy. We intend to expand our search by subjecting leukocytes isolated from breast cancer patients' axillary lymph nodes (ALNs) to Phosflow and observe whether the fold induction of STAT1-pY701 significantly decreases or increases and possibly, extend it to tumor infiltrating leukocytes (TILs) depending on the number of cells we can isolate.
- Determine the mechanism(s) by which IFN signaling is hindered. Two approaches will be used to address this issue:
    - First, a step-by-step approach to look at phosphorylation events upstream from STAT1, such as JAK1, JAK2, TYK2, and IFN receptors. Currently, we are optimizing protocols to use with a new system, Firefly 3000. Firefly 3000 has the ability to quantitate and analyze proteins from a small amount of material. Once optimized, we will be able to explore and possibly identify mechanistic defects in the immune and tumor cells isolated from breast cancer tumors, tumor-draining lymph nodes (TDLNs), and/or peripheral blood leukocytes.
    - Our second approach is to determine whether JAK/STAT signaling cascades in other pathways are perturbed in some manner. We decided to utilize Phosflow and stimulate PBMCs with IL-6 and IL-2. The target cells for IL-6 stimulation are T cells and B cells, whereas, the target cells for IL-2 stimulation include T cells, B cells, and NK cells. IL-6 and IL-2 were chosen because both of these stimuli use JAK/STAT pathways and we would like to determine if similar players in the IFN signaling cascade are involved in down regulation (or up regulation) of response in other pathways.

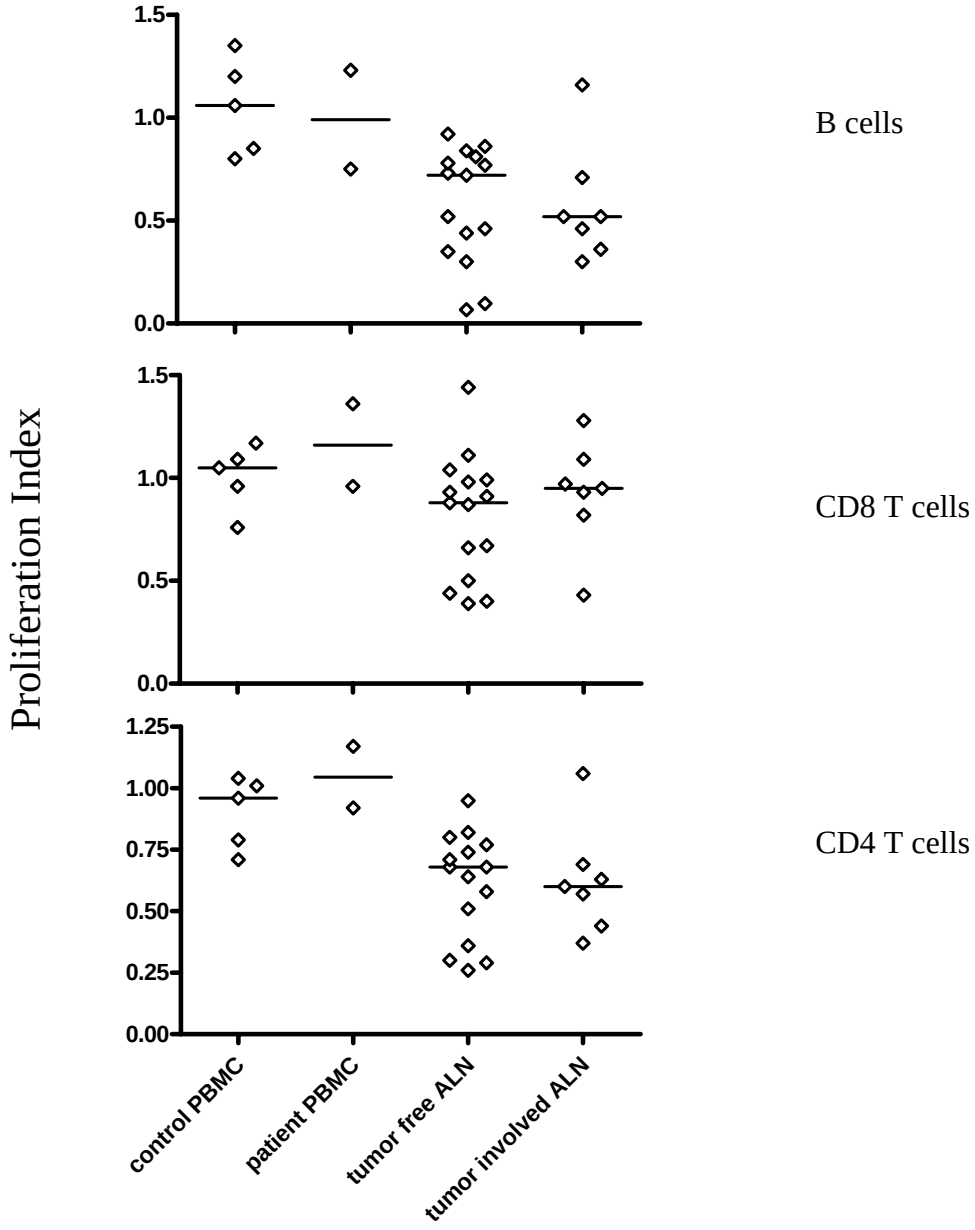

Figure A1. Isolated immune cells were labeled with CFSE and stimulated with phorbol esters/Ionomycin for 115hour. Cell divisions were analyzed by FACSAria and cell proliferation analysis was performed by flowjo. Proliferation capability of B cells, CD8 T cells, CD4 T cells for 5 healthy control blood samples, 2 patient blood samples, 16 tumor free lymph nodes, 7 tumor involving lymph nodes are illustrated in separate scatter columns. Y axis indicates division index, the average number of divisions a cell has undergone. Medians are indicated by the bar in each scatter column.

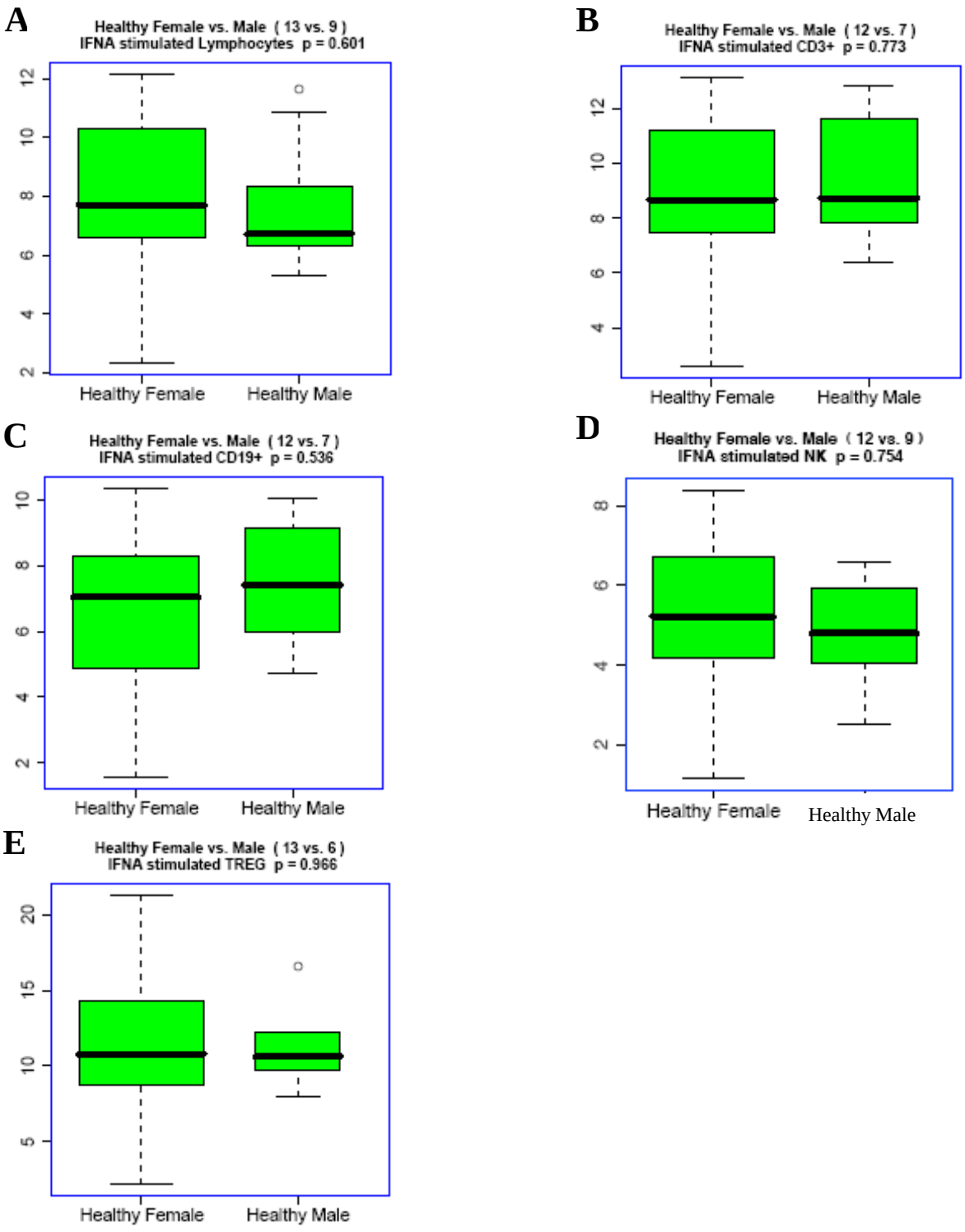

Figure A2. IFN-α-Stimulated fold change in pSTAT1-Y701 of PBMC subsets from healthy female and healthy male donors with corresponding p-values as measured by Phosflow. A: Lymphocytes, B: CD3 T cells, C: CD19 B cells, D: CD16 Natural Killer cells, and E: T regulatory cells

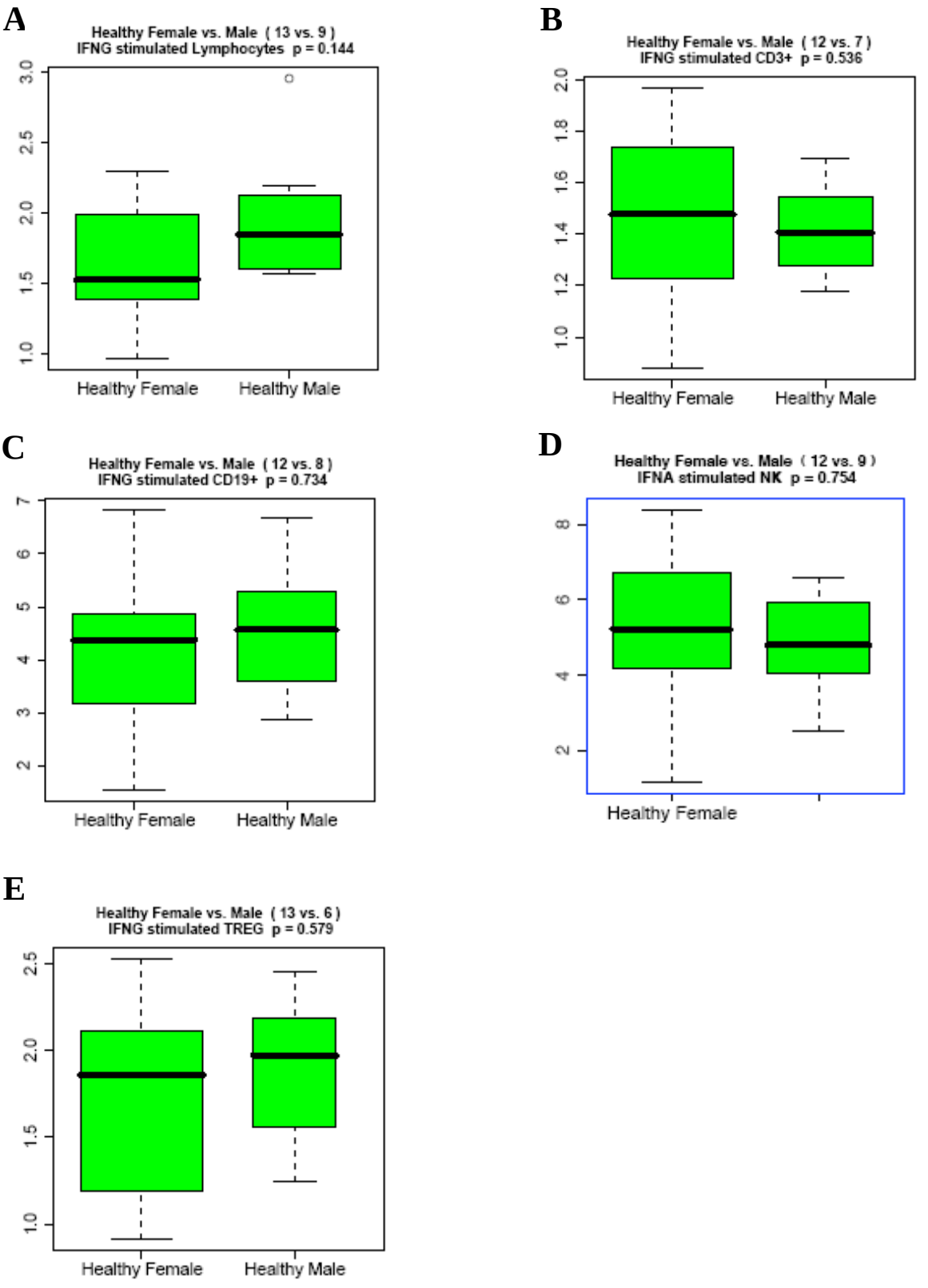

Figure A3. IFN-γ-Stimulated fold change in pSTAT1-Y701 of PBMC subsets from healthy female and healthy male donors with corresponding p-values as measured by Phosflow. A: Lymphocytes, B: CD3 T cells, C: CD19 B cells, D: CD16 Natural Killer cells, and E: T regulatory cells

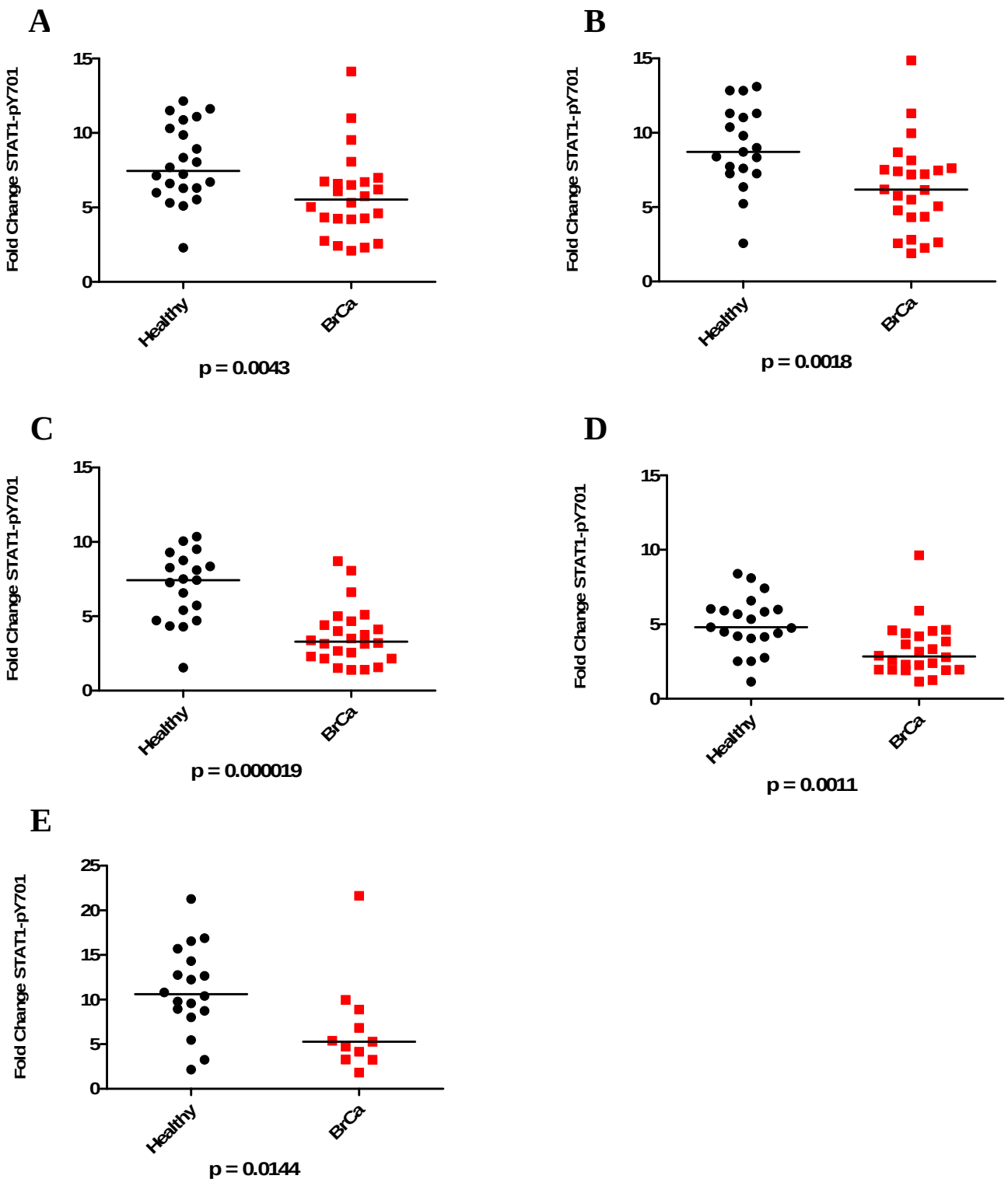

Figure A4. IFN-α-Stimulated fold change in STAT1-pY701 in PBMC subsets from healthy (●) and breast cancer patients (BrCa ■) with corresponding p-values as measured by Phosflow. PBMC subsets were gated based on surface markers measured by FACS. A: Lymphocytes, B: CD3 T cells, C: CD19 B cells, D: CD16 Natural Killer cells, and E: T regulatory cells.

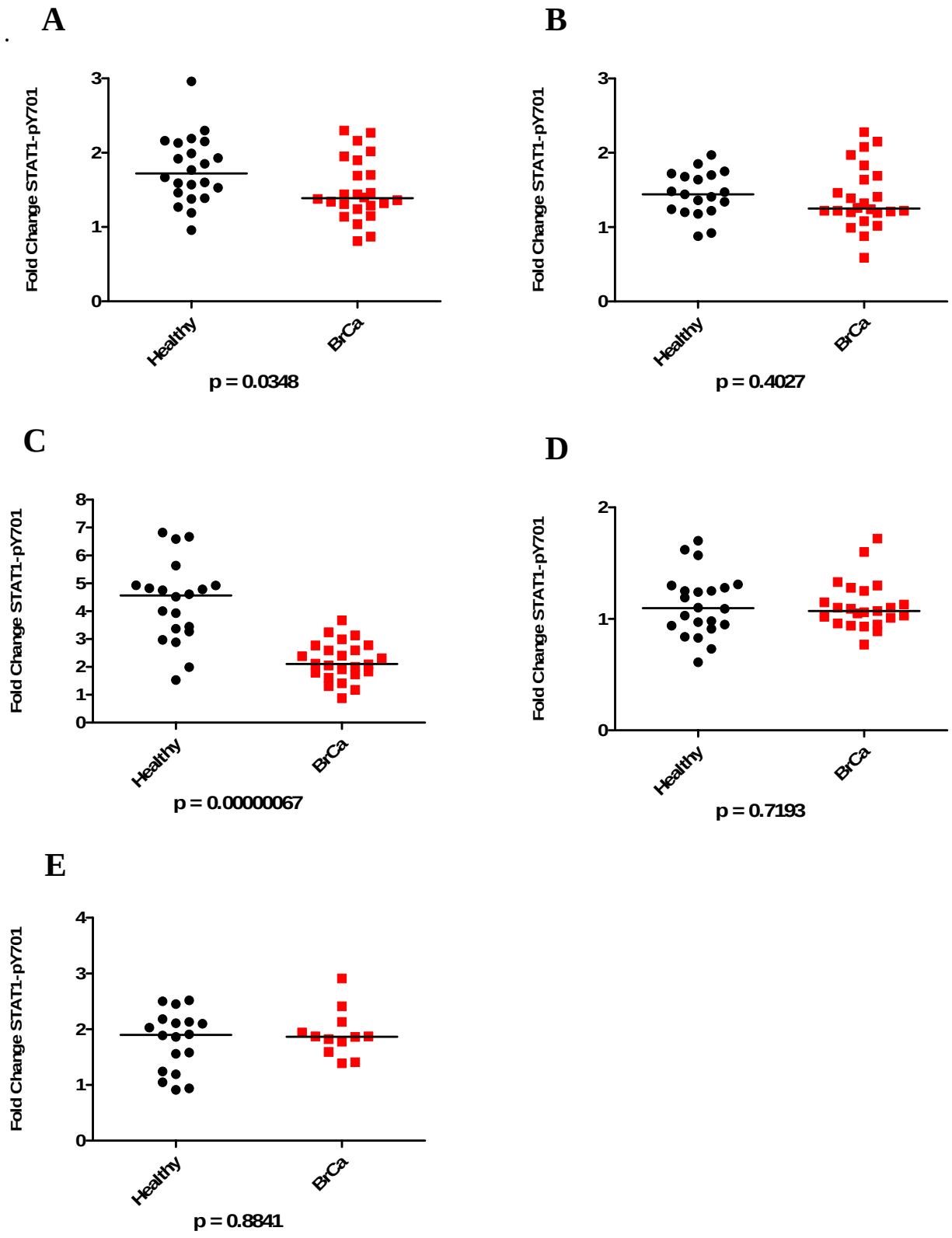

Figure A5. IFN-γ-Stimulated fold change in STAT1-pY701 in PBMC subsets from healthy (●) and breast cancer patients (BrCa ■) with corresponding p-values as measured by Phoslfow. PBMC subsets were gated based on surface markers measured by FACS. A: Lymphocytes, B: CD3 T cells, C: CD19 B cells, D: CD16 Natural Killer cells, and E: T regulatory cells

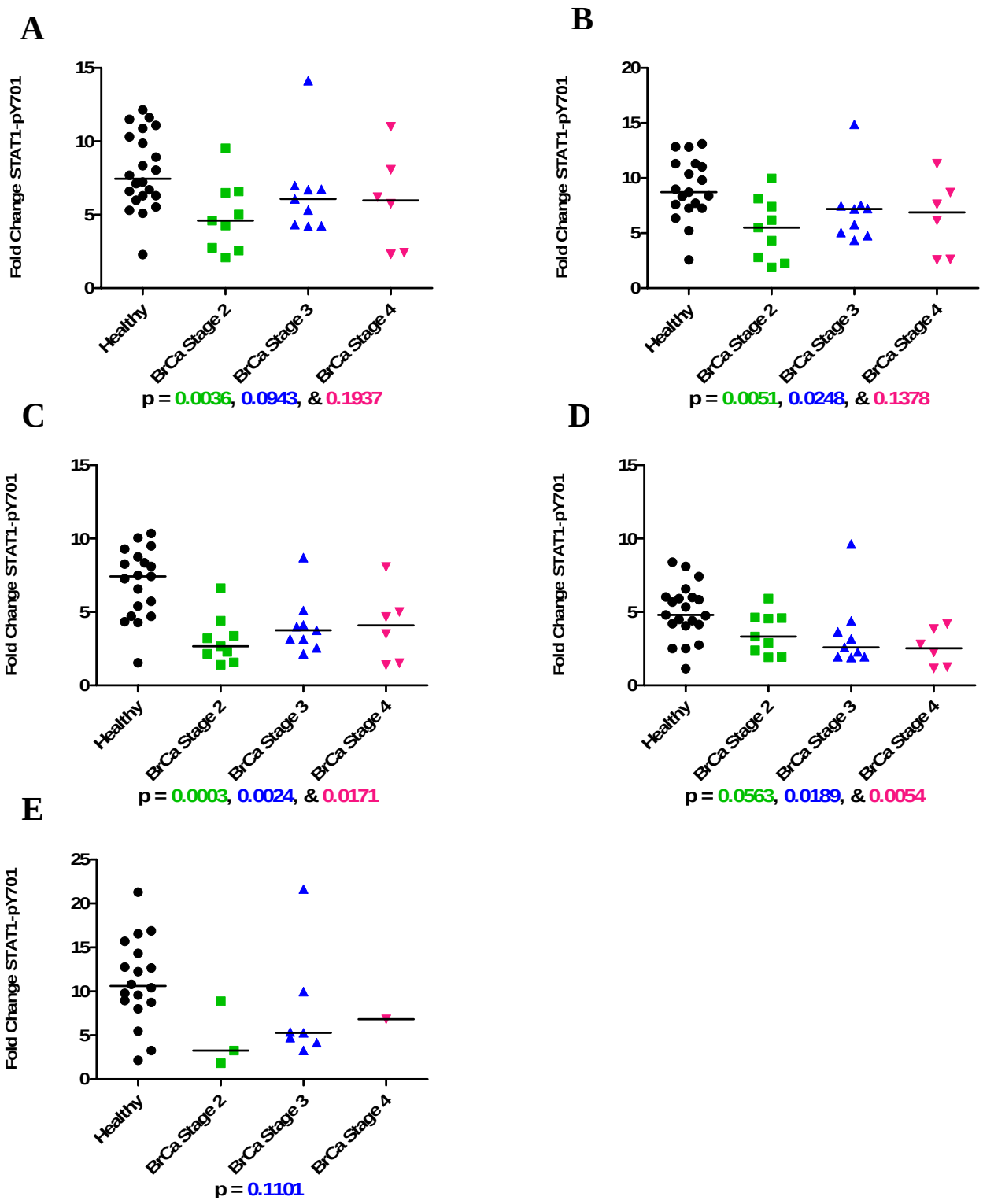

Figure A6. IFN-α-Stimulated fold change in STAT1-pY701 in PBMC subsets from healthy (●)and breast cancer stages (2- ■, 3- ▲ , 4- ▼) with colored corresponding p values. PBMC subsets were gated based on surface markers measured by FACS. A: Lymphocytes, B: CD3 T cells, C: CD19 B cells, D: CD16 Natural Killer cells, and E: T regulatory cells.

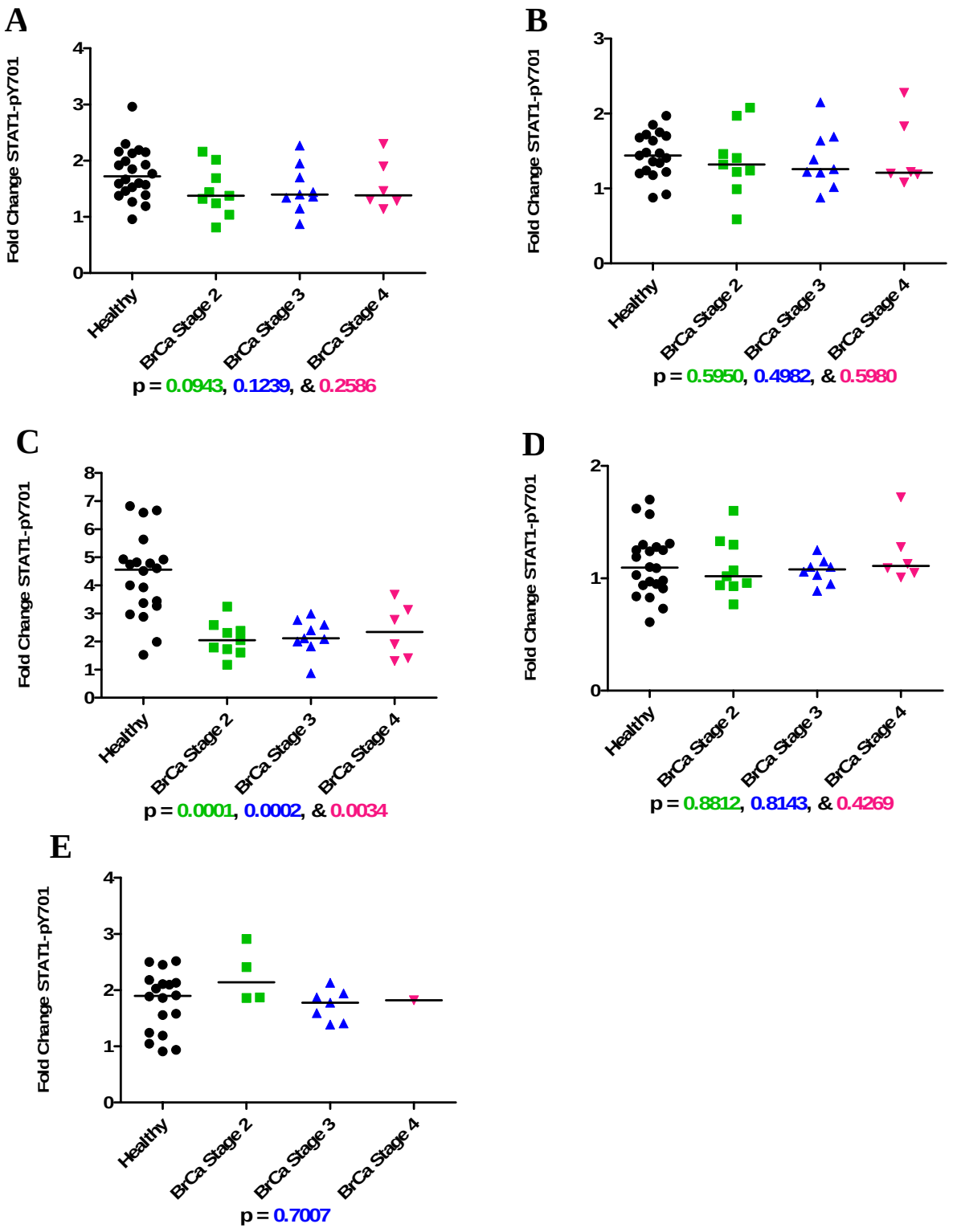

Figure A7. IFN-γ-Stimulated fold change in STAT1-pY701 in PBMC subsets from healthy (●)and breast cancer stages (2- ■, 3- ▲, and 4- ▼) with colored corresponding p values. PBMC subsets were gated based on surface markers measured by FACS. A: Lymphocytes, B: CD3 T cells, C: CD19 B cells, D: CD16 Natural Killer cells, and E: T regulatory cells.

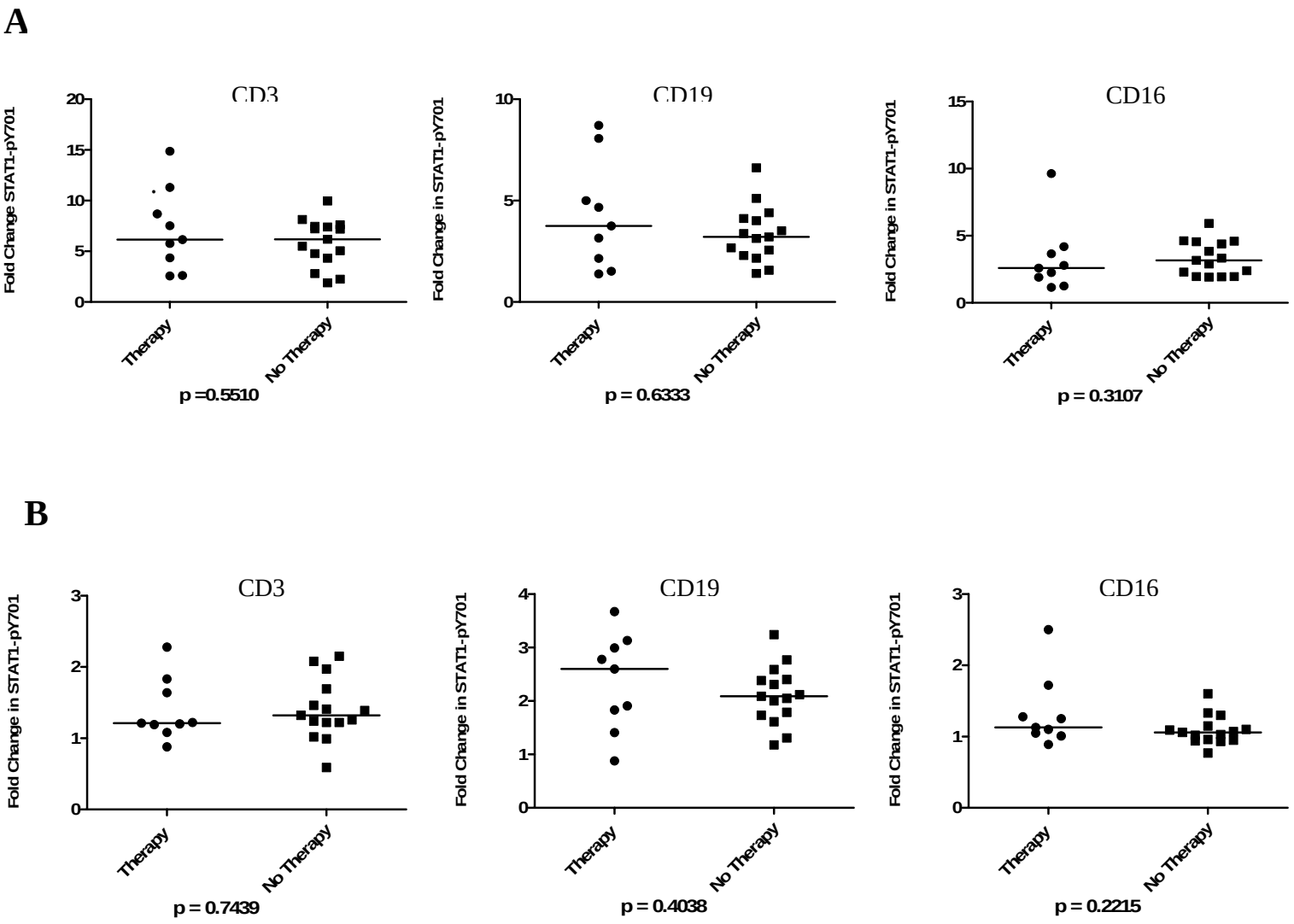

Figure A8. IFN stimulated fold change in pSTAT1-Y701 for PBMCs of breast cancer patients who received neo-adjuvant or adjuvant therapy (therapy ●) compared to breast cancer patients who did not receive either therapy(no therapy ■) as measured by Phosflow: A) IFN-α-stimulated PBMC subsets for CD3 T cells, CD19 B cells, and CD16 Natural Killer cells with corresponding p-values. B) IFN-γ-stimulated PBMC subsets for CD3 T cells, CD19 B cells, and CD16 Natural Killer cells with corresponding p-values.

Personnel: Lee, Johnson, Dirbas, Schwartz, Yu, Simons.

B. Microarray analysis of immune and tumor cells independently

Originally proposed in SOW:
1. Microarray analysis of gene expression of purified tumor and immune cells, isolated from fresh tumor or TDLN samples, and peripheral blood mononuclear cells (PBMC) from breast cancer patients. (months 6-60)
2. Detailed analyses of gene expression data focusing on gene networks and cross-talk between tumor and immune cells. (months 12-60)

This project utilizes a systematic approach to study the dynamics between breast cancer and the immune responses by directly comparing the gene expression patterns from TDLNs with the tumor site and peripheral blood. An increasing number of studies have used microarray to profile breast tumor specimens, which in fact represent heterogeneous cell populations consisting of tumor cells and tumor infiltrating immune cells. Our strategy is to profile purified tumor and immune cells independently, isolated from tumors and/or TDLNs.

1. Summary of sample composition for microarray analysis

Our initial set of gene expression data will comprise up to 225 samples collected from 30 newly diagnosed breast cancer patients. These samples include immune cells and/or tumor cells from peripheral blood, breast tumor tissues, and TDLNs (tumor free or tumor involving). Of these, a total of 13 complete patient sample sets will include tumor cells and their paired immune cells from tumor tissues, TDLNs, and blood. These sample sets will allow us to compare the gene expression patterns across all three anatomical compartments.

2. Microarray platforms

A variety of microarray platforms are now available for whole genome gene expression profiling. Initially we proposed to use two microarray platforms for this study, Affymetrix Human Genome U133 (HG-U133) Set and Agilent Whole Genome Oligo Microarray 44K. There is no universally accepted standard for comparing data from different platforms, or even within the same array types. As mentioned in the previous progress report, we attempted to develop protocols to compare microarray data across groups, labs and platforms. However, due to the lack of coherency in array technologies, confusion in interpretation of data within and across platforms has often been the norm, and studies of the same biological phenomena have, in many cases, led to contradictory results. Furthermore, Agilent has replaced the Agilent Whole Genome Oligo Microarray 1×44K with 4×44K, which makes the cross platform comparison more difficult. In a pilot study we found different gene expression pattern of reference RNA samples between Agilent 1×44K and 4×44K. More importantly, the total RNA requirement (200 ng) for multiple platforms will bias the selection of patient samples against small breast tumor tissues and/or with less immune cell infiltrations. Hence, we have decided to go with a single microarray platform for the entire project.

Tecan recently developed the QuadChamber for fully automated processing of Agilent's new (4×44K) 4-plex gene expression arrays. We performed pilot studies comparing Agilent's

1×44K and 4×44K and found this automated system ensures high quality processing with minimal slide handling, minimal ozone exposure, excellent reproducibility and bubble-free hybridization. Agilent's 4-plex microarrays concentrate sample hybridization, so provide enhanced sensitivity and allow the detection of even very low abundance transcripts. Therefore, Agilent's new 4-plex Whole Genome Oligo Microarray (4×44K) and Tecan's automated hybridization system will be used for this project.

3. RNA Amplification

Previously optimized protocol requires 100 ng of total RNA as starting material. Various technologies are now available to allow the use of very small amounts of RNA. To take advantage of this, we compared the RNA amplification protocols using Amino Allyl MessageAmp™ II aRNA Amplification Kit (Ambion, Inc) with TrueLabeling-PicoAMP™ Kit (SuperArray). The TrueLabeling-PicoAMP™ kit is able to amplify and label antisense RNA from picogram quantities of total RNA. Table 2 lists the typical yields obtained using TrueLabeling-PicoAMP™ kit based on the number of immune cells and tumor cells. High sensitivity quality control of amplified RNA samples is carried out using the RNA 6000 Nano LabChip kit and 2100 Bioanalyzer (Agilent). Using this protocol, we determined that a minimum of 5000 immune cells and 3000 tumor cells are sufficient for Agilent 4-plex microarray. This produces about 6μg of aminoallyl-cRNA with minimal non-specific amplification product, which is enough for 3-4 arrays.

Table 2. Yields of cRNA obtained using TrueLabeling-PicoAMP™ kit (2-round amplification)

Cell No.	from immune cells	from tumor cells
2,500	8μg	5μg
5,000	5μg	15μg
15,000	10μg	30μg
20,000	15μg	35μg
25,000	25μg	25μg
50,000	50μg	55μg

4. Batch difference

The initial set of microarray analysis comprises up to 450 arrays, with two arrays for each sample. The maximal capacity of Tecan automated hybridization system is 48 arrays per batch. To minimize batch difference we might encounter, we identified three major factors that could potentially introduce batch difference: RNA amplification, Cy3/Cy5 labeling and hybridization. We performed a set of microarray experiments designed to quantify the influence of the three factors mentioned above. Microarray analysis was carried out using total lymphocytes reference samples in various hybridization/amplification/labeling batches (a total of 14 arrays). Our data suggest that the amplification batch difference is relatively larger than the labeling and hybridization batch difference. Of particular note, the amplification batch difference is due to different amount of input RNA.

Our samples have various numbers of cells, ranging from 2,500 to 1 million. Although standardization of input RNA material will minimize bias introduced by amplification, the quality of the whole data set might be jeopardized by limiting the input RNA to the smallest

amount available. Based on the yields of aminoallyl-cRNA using the TrueLabeling-PicoAMP^{TM} kit, we decided to use as much input total RNA as is available for samples with less than 50,000 cells. This will maximize accurate gene expression profile representation. The amplification reaches the maximal efficiency with a cell number of 50,000. Increase of input RNA thereafter unnecessarily expends limiting reagents at no additional yield advantage. Therefore, total RNA is quantitated using Ribogreen (Invitrogen) method for samples with cell number above 50,000 and 1 ng of input RNA is used for amplification.

5. Reference RNA

Agilent's two-color hybridization allows comparison of two samples labeled with different fluorescent dyes on the same microarray. Normalized signals are expressed as the ratio of signals from Cy5 experimental and Cy3 reference probes, or vice versa. Use of a common reference sample across multiple experiments provides reliable data comparison. A reference sample should provide a hybridization signal at as many probe elements as possible. We carried out a pilot study to compare the performance of our in house total lymphocyte reference RNA and Stratagene's Universal Human Reference RNA. Comprised as a collection of RNA pooled from ten cell lines, the Stratagene's UHR RNA has broader gene coverage and provides us the ability to cross compare data sets from public domain. Stratagene's UHR RNA is used for the first set of gene expression analysis.

6. Protocols developed for Agilent Whole Genome Oligo Microarray 4×44K

Total RNA is isolated through Trizol method and amplified in two consecutive rounds using TrueLabeling-PicoAMP^{TM} kit, followed by the Cy3/Cy5 labeling (Amersham Biosciences Corp.) and Tecan automated hybridization according to the Agilent technical manual.

Personnel: Lee, Holmes, Johnson, Dirbas, Yu, Simons. **A third PhD postdoctoral fellow with expertise in bioinformatics, data integration and analysis would greatly enhance the success of this project.**

C. Epigenetic dysregulation

> Originally proposed in SOW:
> Assess alterations in epigenetic control of gene expression in immune cells (due to direct effects of tumor cells or to the general cancer state) isolated from fresh tumor or TDLN samples, and peripheral blood mononuclear cells (PBMC) from breast cancer patients. This will be done using proprietary technologies from Orion Genomics – Methylscope and Methylscreen.

While this remains a promising line of investigation, these analyses require substantial amounts of patient materials. Our experience continues to suggest that we do not have sufficient numbers of immune cells recovered from patient specimens to fully support these higher risk analyses. This stems from the current trends in the surgical management of breast cancer patients of removing fewer lymph nodes and patients with smaller tumors being detected. Both of these trends lead to smaller and fewer samples from breast cancer patients

being available for research purposes, necessitating the need for us to optimize all of our assays and focusing on the highest yield experiments. Even with our best efforts, we have barely sufficient patient materials for immunological and gene expression analyses – we simply do not have sufficient patient materials to pursue this analysis. Hence, we will remove this exploratory analysis from our project going forward. Neither funds nor personnel effort was budgeted for this exploration, so this will not alter our overall project plans going forward.

D. Analyzing the geometric relationships and interactions between cancer and immune cells in tumors and TDLN

> Originally proposed in SOW:
> 1. Generate high-resolution images of tumor and TDLN sections. (months 0-60)
> B. Develop algorithms to identify cells/cell types and assign coordinates. (months 0-60)
> 2. Develop algorithms to assess the spatial arrangement and grouping of tumor and immune cells with respect to each other that may have biological significance. This will be done in collaboration with a Stanford mathematics professor, Dr. Doron Levy, using advanced image analysis and computational geometry techniques. (months 0-60)

Archived samples of tumor and TDLN from breast cancer patients with at least 5 years of clinical follow-up data are being analyzed. Tumor and immune cell markers are identified via immunohistochemical (IHC), immunofluorescence (IF) staining, and in-situ hybridization (ISH). Images are being acquired using a high-resolution, automated imaging system (Olympus and Ludl) with a special spectral imaging system (Nuance^{TM}). Acquired images are then analyzed with our custom image analysis software Gemident. This software uses spatial statistics and machine learning algorithms to identify cells, cell types, and assign coordinates. We are also developing algorithms to assess the spatial arrangement and grouping of tumor and immune cells. By performing *in situ* analysis of tissue, our goal is to understand the mechanisms of cancer development by characterizing the spatial interactions between cell types. This is done in collaboration with Stanford statistics professor, Dr. Susan Holmes, who has expertise in novel image analysis and computational geometry techniques. Over 50 immune and tumor markers will be eventually be assessed within tumor and TDLN sections.

Thus far, we have optimized 3-color IHC staining combinations to concurrently visualize breast cancer cells (via cytokeratin AE1/AE3) and various immune cells within tumor and TDLN sections. Key accomplishments of this year include the optimization of 3-color IHC staining protocols and integration of the automated imaging system that yield high-resolution images (figure D1 and D2), and completion of our custom image analysis software that enables us to identify each cell type, its location, and enumerate the total numbers of tumor and immune cells within each section (figure D3).

We have initiated large-scale spatial data analysis based on the automated cell type identification performed by our software. To date, our statistical analysis has involved

quantifying the inter-point distances between cells (figure D4a). We have begun to study the geometry of cancer cell intensity by mapping regions of dense tumor intensity (figure D4b). Understanding these cellular spatial patterns will allow us to understand the mechanisms of cancer development.

The exploratory statistical analysis of cell location data enables us to build a spatial picture of the data. Both the individual cell populations of homogeneous type (T cells, dendritic cells, cancer cells, others) and the interaction between these populations inform us to the dynamics that lead to such a configuration.

For the time being we are trying to model the underlying processes both with marked point process models and clustering detection procedures. We are using R and many packages available at the Comprehensive R Archive Network (http://cran.r-project.org/). For example, DCluster is a package for the detection of spatial clusters of diseases, that can also be used to identify and validate cell clustering. The spdep R package provides basic functions for building neighbor lists and spatial weights, tests for spatial autocorrelation for areal data like Moran's I statistic, and functions for fitting spatial regression models, such as Spatial Autoregressive (SAR) and Conditional Auto Regressive (CAR) models. These models assume that the spatial dependence can be described by known weights.

While this work is in progress, we are being to uncover interesting spatial relationships between tumor cells, immune cells, and tumor-immune cells. More importantly, these relationships can be quantified and used in downstream statistical analyses, including relationship with clinical parameters and outcomes.

Figure D1. Spectral unmixing of a triple-stained lymph node section by Nuance™. Chromogens used were Vulcan Fast Red (cytokeratin (tumors), red), DAB (CD1a(+)-dendritic cells, brown) and Ferangi Blue (CD3(+)-T cells, dark blue). Cellular nuclei were counterstained with hematoxylin (light blue). *A,* An original RGB image of a part of a tissue section. *B,* Images resulting from unmixing of the spectral signals of each chromogen and counterstain. *C,* Reconstructed image with pseudo-colors that allowed a greater distinction of the cell populations as compared to the original image.

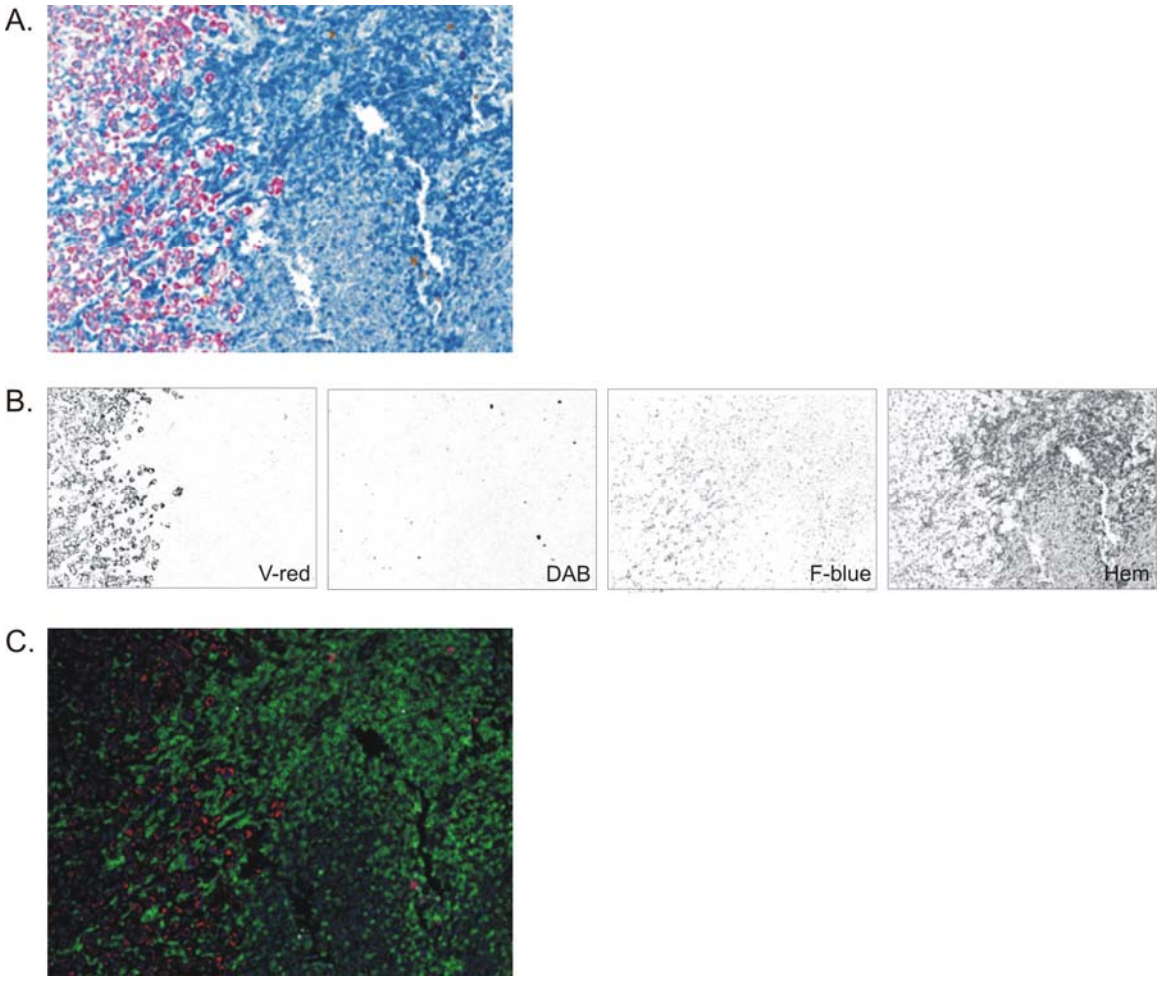

Figure D2. A whole-slide RGB image of a TDLN section taken by Nuance™.

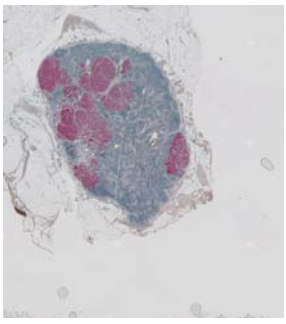

Figure D3. Examples of object identification within complex images by custom image analysis software. *A,* A reconstructed image of a TDLN section with the tissue area marked in green numbers, and stages to be used for phenotype training of the program marked in dark green circles. *B,* Red cells with blue nuclei represent tumor cells, green cells with blue nuclei represent T cells, and blue only cells represent other cell populations. After being trained to recognize each cell phenotype, the program would identify and mark the centroid locations of each identified cell. It then determined the number of each cell phenotype identified in the whole image, and the x-y coordinates that represent the location of each cell in the tissue section.

A.

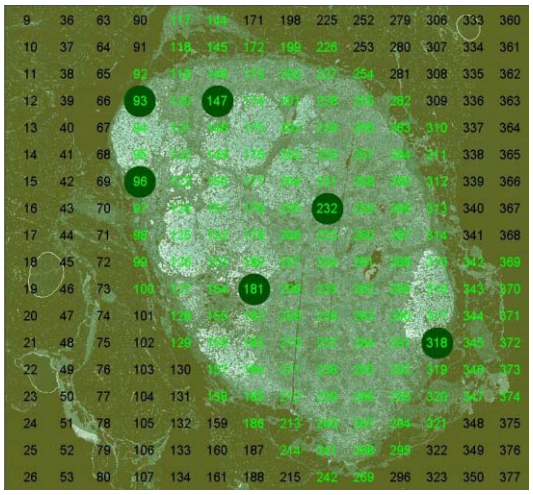

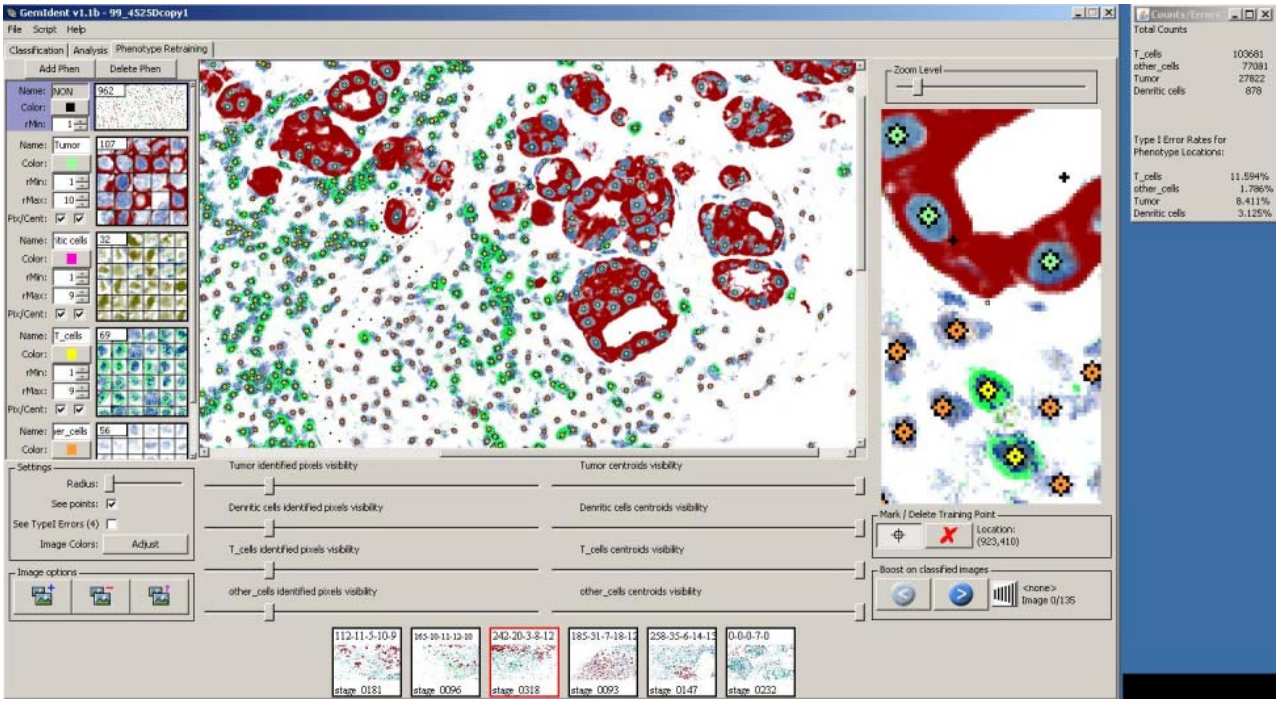

B.

Figure D4. *A.* Bottom (purple) curve denotes the estimated joint probability distribution between a tumor cell to its nearest T-cell neighbor; the top (blue) curve is the theoretical distribution if tumor cells and T-cells were spatially independent. These graphs suggest a significant repulsion effect between tumor cells and T-cells; *B.* estimated tumor cell intensity (number of tumor cells per pixel)

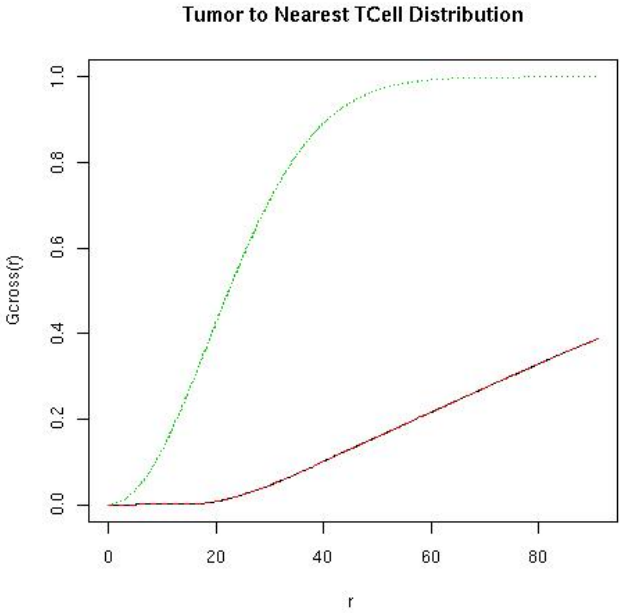

A.

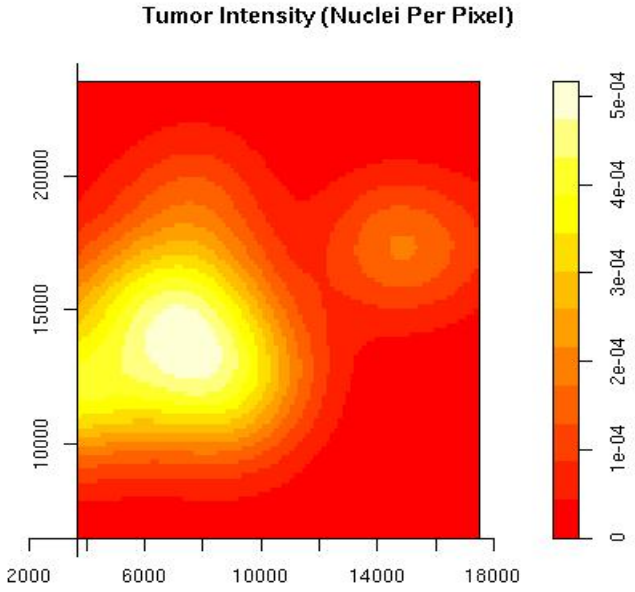

B.

Personnel: Lee, Holmes, Schwartz, Setiadi, Levic, Holmes, Angeles.

E. Synthesizing a useful model of breast cancer through mathematical and computational modeling

> Originally proposed in SOW:
> To integrate our experimental data and observations into a mathematical model to address the dynamics of cancer cells and the immune response in the tumor and lymph node. This will ultimately enable us to perform *in silico* experiments to quickly test novel therapeutic strategies for breast cancer.

As a first step to mathematical modeling of data generated from this project on immune responses to breast cancer, we developed a basic mathematical model for the dynamics of the adaptive immune system during a primary immune response. The main focus of the model is on the T cell-mediated response and particularly on the function of naturally-occurring regulatory T cells. To devise the model, we formulate a system of delay differential equations (DDEs) in which the time delays correspond to the lag between the stimulation and activation of killer T cells or the durations of T cell divisions. Each equation corresponds to a population of cells or molecular signals that contribute to the development of the overall adaptive immune response. In the model, we consider antigen-presenting cells (APCs), three types of T cells (helper, killer, and regulatory), target cells, antigens, and positive and negative growth signals. In addition, we separate the dynamics into two separate compartments, the lymph node and the tissue. The motivation of this paper is to understand the dynamics of self/non-self discrimination of T cells and the mechanisms of immune regulation.

The primary immune response refers to the first encounter of the adaptive immune system with particular non-self antigens. This response begins when a foreign target enters the tissue triggering the innate immune system, which releases a cascade of inflammatory signals. Prior to inflammation, APCs, especially dendritic cells, circulate continually throughout the tissue collecting antigen, both self and non-self, and presenting them on their cell surfaces. Upon encountering inflammatory signals, APCs mature and migrate to the lymph node, where they begin to stimulate naïve T cells that react to the antigens on the APC surfaces.

These interactions trigger a phase of antigen-specific T cell proliferation that lasts about four to ten days depending on the strength of the immune response. During this phase, killer T cells proliferate to thousands of times their original concentration, while helper T cells proliferate to a much lesser extent. Instead, activated helper T cells begin to produce positive growth signal, especially IL-2, to maintain the stimulation of proliferating killer T cells. This dynamic interaction between APCs, killer T cells, and helper T cells in the lymph node leads to a rapid expansion of T cells against specific non-self antigens, while at the same time tolerating normal self antigens, which are generally always present in the body.

At some point, the activated killer T cells begin migrating out of the lymph node to destroy the infecting agent in the tissue. A successful immune response results in the elimination, or at least in a significant reduction, of the virus or other foreign target. Ideally, this response ends in a rapid contraction of the immune cell population before the development of

immunological memory. For the scope of this paper, our modeling does not extend into the dynamics of immunological memory and secondary immune responses. Instead, we focus the regulatory mechanisms that lead to a timely contraction of the immune response as well as an ensured tolerance of self antigen during target elimination.

Regulatory T cells are a relatively recent finding in medical research, so not much is understood about their regulatory mechanisms or their role in the immune system, except that they are essential to prevent auto-immune disease. However, from recent articles in medical literature, we can understand that naturally-occurring regulatory T cells begin in naïve states and proliferate in an antigen-specific manner in much the same way as other T cells, especially helper T cells. Furthermore, they suppress mature APCs and activated T cells upon contact and secrete negative growth signals to suppress the activity and expansion of other T cells. It is not at first clear whether the regulatory T cell response initiates at the same time as the primary T cell response against foreign target or whether it initiates later. We seek to use our mathematical model to better understand this part of the dynamics.

In addition, we also use the model to gain insight into the differences between lymph node and tissue in driving the immune response. For this purpose, we consider the lymph node and tissue as separate compartments. In the body, these organs provide completely different environments that significantly affect the rate and duration of interactions between immune populations. In particular, the lymph node has a diameter of approximately one to a few millimeters (for mice and humans) and a density of immune cells that is hundreds of times more than that in the tissue. In contrast, the tissue is a much larger region with a size on the order of cubic centimeters and for the most part contains activated T cells rather than naïve T cells and immature APCs rather than mature APCs.

Based on the interactions discussed above, we formulate our model as a system of DDEs. As a fundamental modeling assumption, we assume that cells have only local information from their immediate surroundings and the individual immune cells only exhibit simple responses to stimuli. In other words in our model, individual cells do not possess sophisticated programs that autonomously govern long-term developments, such as the progression between activation, expansion, and contraction phases. Alternatively, we use our model to demonstrate that these temporal phenomena and “collective decisions” can develop from group dynamics emerging from large-scale interactions between various cell populations.

As stated as one of our motivations, we seek to understand the mechanisms of self/non-self discrimination. Recent medical findings show that self/non-self discrimination is not a clear cut, black and white procedure, since the body always has some slightly self-reactive T cells and even predominantly foreign-reactive T cells may have a slight cross-reactivity with self antigen. To this end, we simultaneously consider the immune response to virus-infected cells and the collateral response to self cells.

We demonstrate using numerical simulations that our system can eliminate virus-infected cells, which are characterized by a tendency to increase without control (in absence of an immune response), while tolerating normal cells, which are characterized by a tendency to approach a stable equilibrium population. We experiment with different combinations of T

cell reactivities that lead to effective systems and conclude that slightly self-reactive T cells can exist within the immune system and are controlled by regulatory cells.

Furthermore in our model, we observe the unexpected phenomenon that CD8+ T cell dynamics proceed in two phases. In the first phase, CD8+ cells remain sequestered in the lymph node during a period of rapid proliferation. During the second phase, the CD8+ population emigrates to the tissue, where it quickly destroys the target population. Upon closer inspection, we discovered that the transition between the two phases is mediated by regulatory T cells. During the proliferation phase, APCs that have migrated to the lymph node persistently stimulate helper T cells to secrete positive growth signal, causing killer T cells to continue dividing. As a result, killer T cells tend to remain in the positive signal-rich environment. Once naturally-occurring regulatory T cells have expanded sufficiently to exert a regulatory effect, they induce a transition into the emigration phase.

During the emigration phase, regulatory cells suppress activity in the lymph node by consuming positive growth signal and suppressing APCs and helper T cells. This change in environment causes the majority of killer T cells to stop dividing and start emigrating to the tissue, where they begin to destroy target cells. Since naturally-occurring regulatory T cells begin at a much smaller concentration than non-regulatory T cells, there is an adequate delay between the initiation of the killer T cell response and the regulatory T cell response that allows killer T cells to proliferate sufficiently before emigrating to the tissue. Much later in the immune response, regulatory T cells in the lymph node also emigrate to the tissue and suppress the remaining T cells that are lingering after target elimination.

The two-phase process results in an effective immune response if the transition between phases occurs within an appropriate time window when the killer T cells have expanded enough to be effective but not too much to induce a significant collateral impact on normal tissue cells. From our model, we demonstrate that having too many regulatory T cells causes a premature transition in which too few killer T cells are generated. On the other hand, having too few or no regulatory T cells causes a late transition in which excess killer T cells cause significant damage to self tissue during a prolonged immune response.

Alternatively, an appropriate fraction of regulatory T cells during an immune response causes killer T cells to optimally switch from proliferation to emigration phases. In this situation, target cells are destroyed quickly and effectively. This two-phase dynamic strongly suggests the counterintuitive hypothesis that the presence of regulatory cells may actually expedite target elimination. In fact, in some simulations when there are no regulatory T cells, the emigration of killer T cells begins too late, allowing the foreign target to expand to higher levels before being controlled by the immune response. So even without considering the possible risk to normal self tissue, a small fraction of regulatory T cells seems beneficial for a normal immune response against an infecting agent.

This unexpected observation extends further to implying that the immune system benefits from having a smaller, but significant regulatory T cell response that initiates simultaneously or at most only a couple of days after the start of the non-regulatory immune response. Although it is currently hypothesized that non-regulatory cells are primarily foreign-reactive,

while regulatory T cells are primarily self-reactive, our simulations show that a system with only self-reactive regulatory T cells often does not have an adequate regulatory response to control the expanding non-regulatory T cell population. From this perspective, our model strongly supports the alternative hypothesis that naturally-occurring populations of foreign-reactive regulatory T cells are highly beneficial, and perhaps even necessary, to properly tune the proliferation of primed T cells during the course of a normal primary immune response.

One question that frequently occurs in immune modeling is whether apoptosis alone is enough to regulate the T cells response and lead to a timely contraction.
In a model where all immune activity happens in one compartment, it is possible to have an immune response that contracts shortly after the absence of foreign-antigen. The principal shortcoming may be that the initial immune response may not initiate as quickly as desired. This discrepancy may be accounted for by assuming that T cells have a slower death rate upon initial activation, but then transition to a higher death rate after several days due to an internal mechanism. However, regardless of what can be demonstrated in a one-compartment model, medical literature makes it clear that most T cell proliferation happens in the lymph node.

In our two-compartment model, we discover that apoptosis alone is not enough to ensure a timely contraction, because of the vastly different dynamics of the lymph node. In the lymph node, the high concentration of immune cells allows the rapid stimulation and expansion of almost every antigen-reactive T cell. However, these T cells remain quarantined in the lymph node and do not easily perceive or respond to changes in the tissue compartment. Furthermore, the high concentration of APCs, T cells, and positive growth signal initiates a very strong positive feedback loop that needs to be broken to initiate the contraction cycle. The presence of regulatory T cells not only provides a mechanism of breaking the positive feedback loop, but it also ensures that the non-regulatory T cell population contracts faster than would happen due to a passive decay from a constant natural death rate.

In addition to the hypotheses discussed above, our model confirms the current standard paradigm that a self-tolerant system must have a mechanism of central tolerance (i.e., naturally-occurring regulatory T cells that are present before infection). Indeed, without a sufficient level of naturally-occurring T cells, the immune response will nearly always cause very high levels of damage to self tissue while eliminating the foreign target.

Going forward, this model of basic immune regulatory mechanisms will be expanded to include tumor cells. Data generated from this project will be added to the model. These efforts will begin in year 3, but will be most fruitful in years 4 and 5 when substantial amounts of data will be available for input into this model.

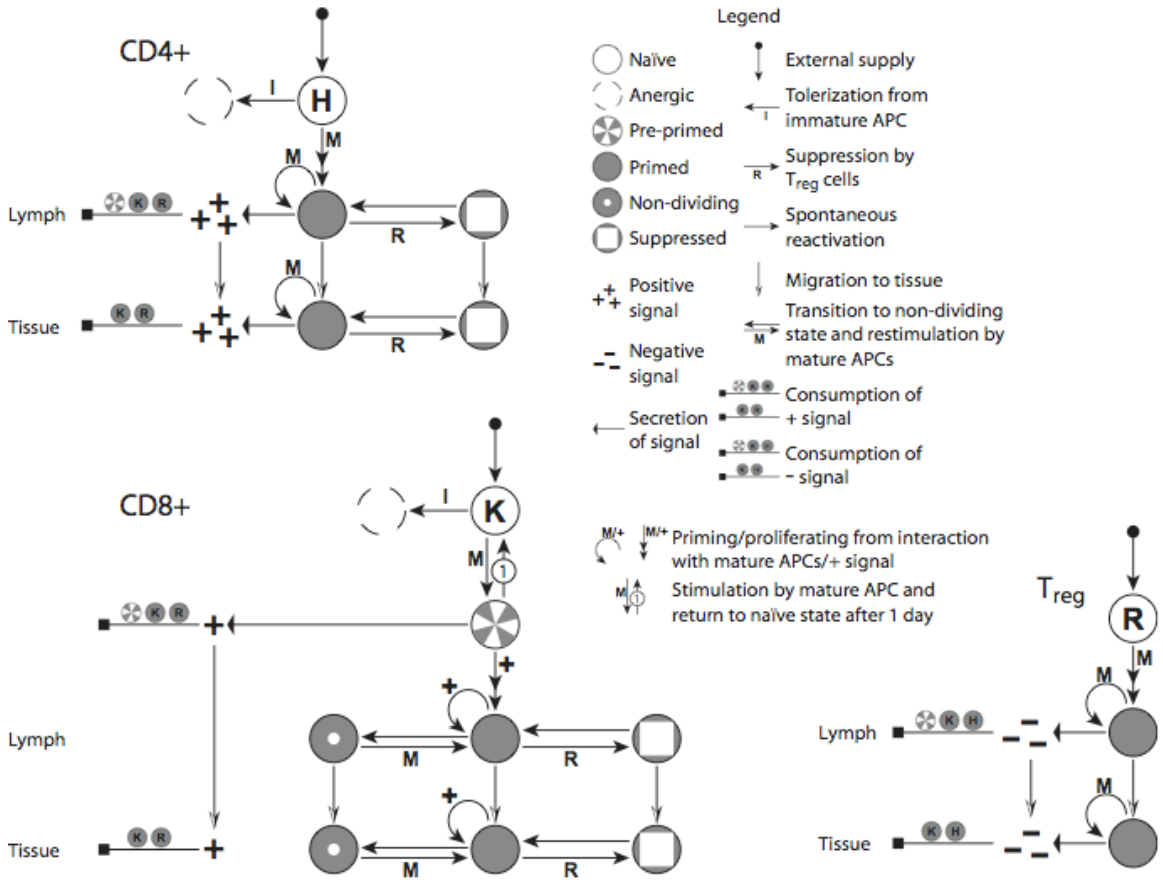

Figure E1: The model. A comprehensive T cell diagram. H, K, and R denote CD4+, CD8+, and regulatory T cells, respectively. Every cell perishes at a natural death rate, which are not shown. Furthermore, all active T cells take up negative signal, which decreases their reaction probabilities.

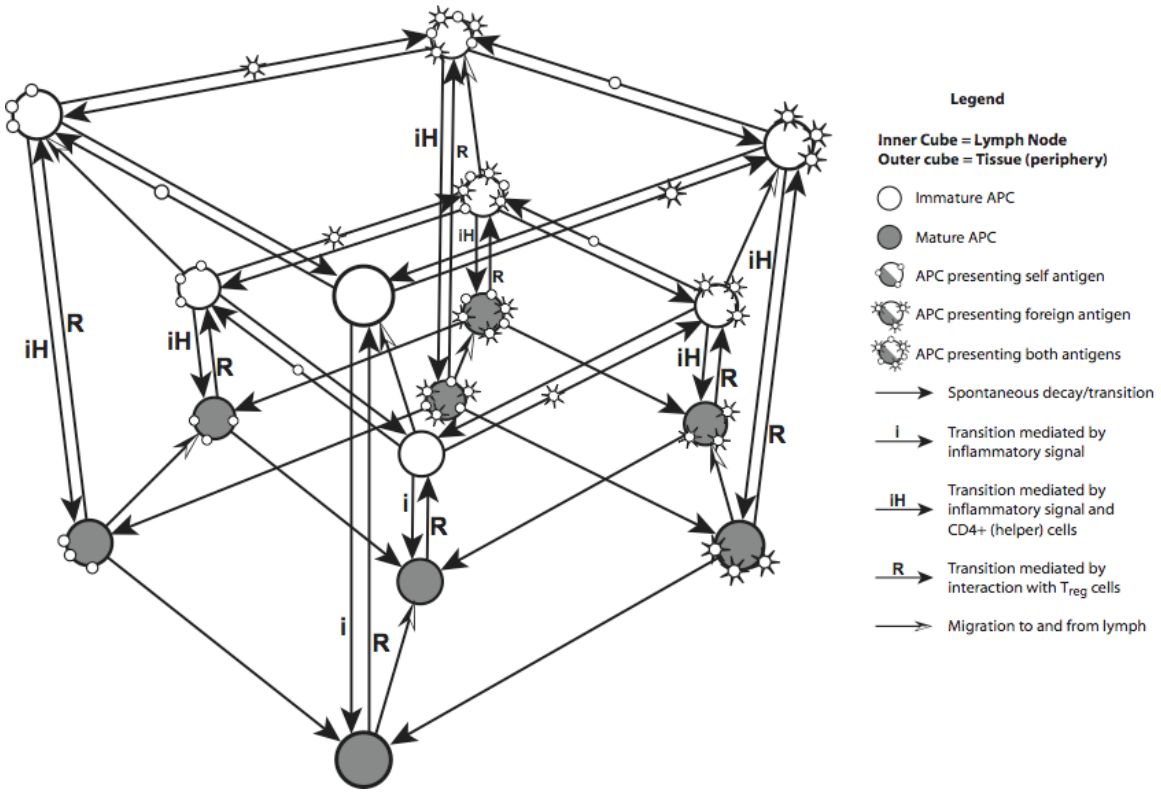

Figure E2: The model. A comprehensive APC diagram. The inner cube corresponds to the lymph node. The outer cube corresponds to the tissue.

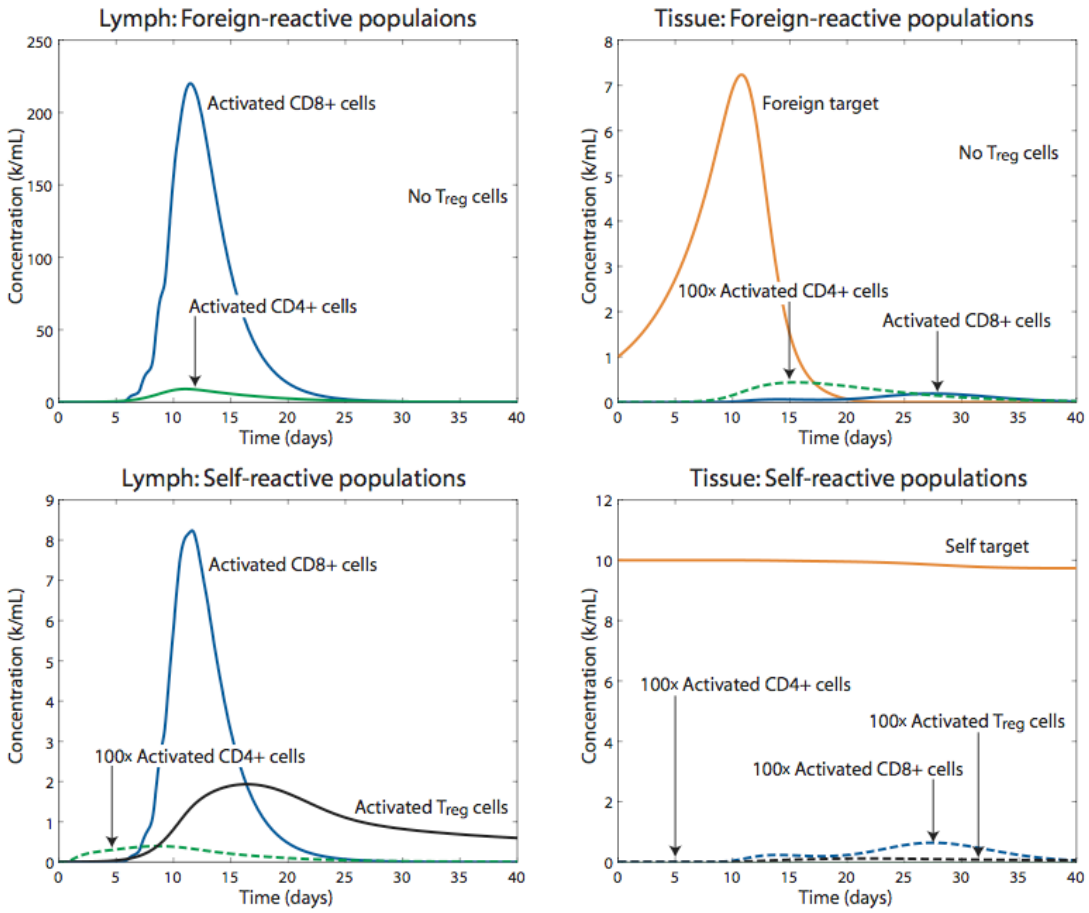

Figure E3: Simulation results: well-regulated immune response without foreign-reactive regulatory cells

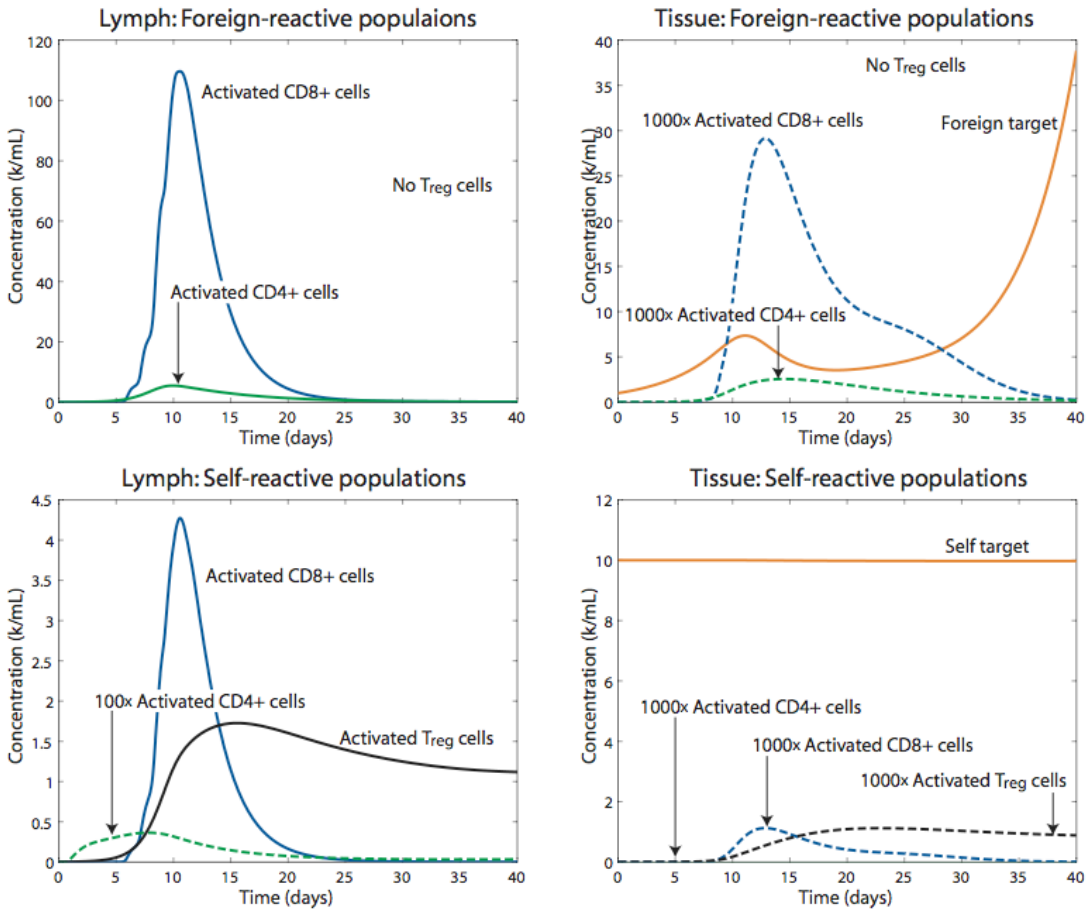

Figure E4: Simulation results: over-regulated immune response without foreign reactive regulatory cells

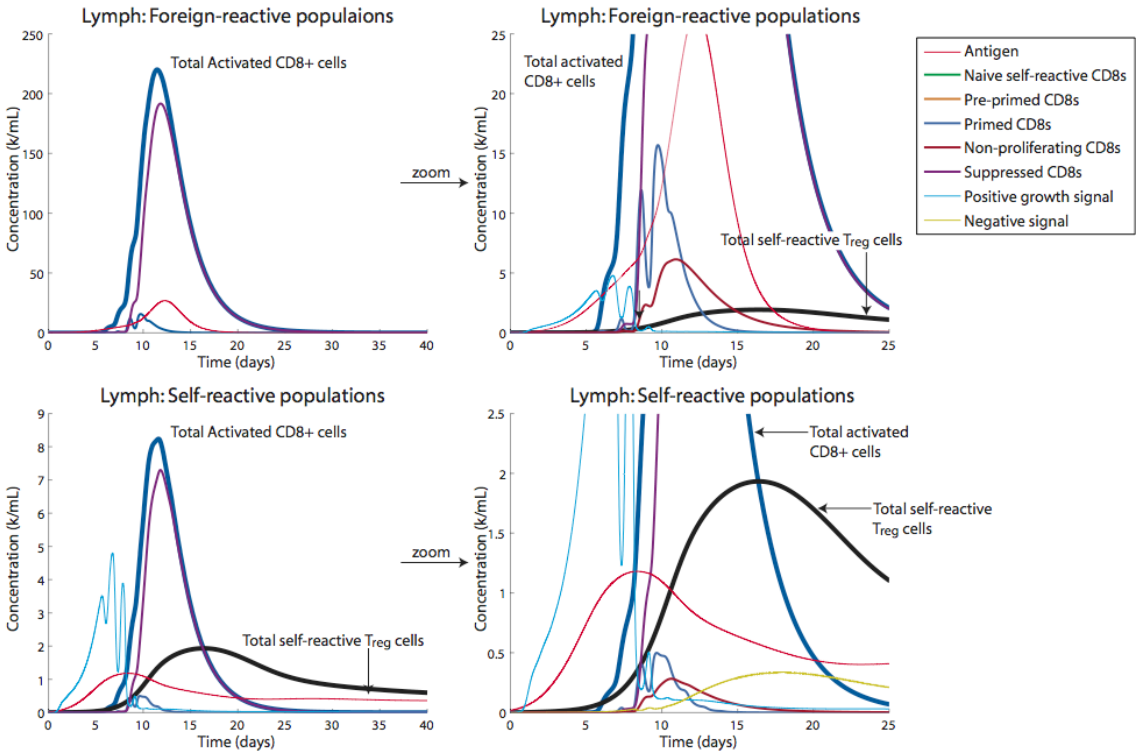

Figure E5: Simulation results: CD8+ cells and signals and the lymph node

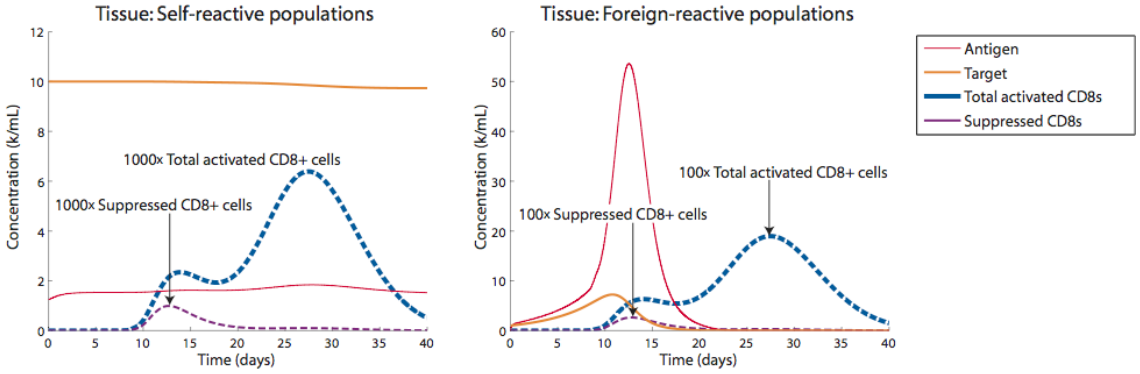

Figure E6: Simulation results: target, antigen, and CD8+ T cells in the tissue

Personnel: Lee, Levy, *Kim. *Kim was a PhD graduate student in mathematics who was involved in this project. He recently completed his PhD and has moved on to a postdoctoral position elsewhere. **A third PhD postdoctoral fellow with expertise in bioinformatics, data integration and analysis would greatly enhance the success of this project.**

Overall Personnel

1. Peter P. Lee, MD – project PI (50% effort on EHSA).
2. Erich Schwartz, MD, PhD – Stanford Pathology (no salary requested on EHSA).
3. Denise Johnson, MD and Fred Dirbas, MD – Stanford Surgical Oncology (no salary requested on EHSA).
4. Susan Holmes, PhD – Stanford Statistics (1 month per year, as 33% of 3-month summer period).
5. Doron Levy, PhD – Stanford Mathematics (Year 1: 1 month per year, as 33% of 3-month summer period; Years 2-5: 2 months as 66% of summer period). Professor Levy recently relocated to the University of Maryland but will stay involved in this project.
6. HongXiang Yu, PhD - post-doc 1, 100% effort on EHSA – immunological and microarray studies.
7. Francesca Setiadi, PhD - post-doc 2, 100% effort on EHSA – histology studies, data analysis.
8. Rudy Angeles, graduate student (Stanford Statistics), 100% effort on project but funded by fellowship – image analysis and data integration.
9. Diana Simons - research assistant 1, 100% effort on EHSA – to aid in immunological, histology, and microarray studies.
10. Edina Levic - research assistant 2, 100% effort on EHSA – to aid in patient enrollment/consent, sample acquisition and processing.
11. Peter Kim, graduate student (Stanford Mathematics), 100% effort on project but funded by fellowship – data integration and mathematical modeling. Peter recently completed his PhD and has moved on to a postdoctoral position elsewhere.

KEY RESEARCH ACCOMPLISHMENTS:

- Recruited 93 breast cancer patients into this study – acquired tumor, TDLN, and blood samples for analyses.
- Finalized protocols to maximize recovery of immune cells and tumor cells from tumor and lymph node specimens.
- Optimized methods for analysis of fresh and archive samples by flow cytometry, function assays, and DNA microarray analysis to study immune and tumor cells within tumor and TDLN specimens.
- Preliminary analysis suggests that there are functional abnormalities in B cells, CD8 T cells, and CD4 T cells from TDLNs as compared with peripheral blood.
- Demonstrated a defect in IFN signaling in peripheral blood lymphocytes from breast cancer patients.
- Over 50 samples have been processed for gene expression analysis by microarrays, which is on-going. We expect to see interesting results in year 3.
- Optimized 3-color immunohistochemical (IHC) staining panels for analysis of archived tumor and TDLN specimens. Over 100 samples are being analyzed.
- Developed custom image analysis software (Gemident) to identify each cell, cell type, location, and relate cell populations by distances and geometric patterns.
- Developed a mathematical model of immune regulatory mechanisms as a first step to modeling immune responses to breast cancer.

Outline of the project plan for the next 12 month

- Continue recruiting patients into study and acquiring samples.
- Continue functional assays of lymphocytes from tumor, TDLNs, and peripheral blood.
- Complete microarray analysis of patient sample sets. Each set includes tumor cells, tumor infiltrating immune cells, immune cells from TDLN, and immune cells from blood.
- Analyze IFN signaling in lymphocytes from TDLNs and tumor, as compared to those in peripheral blood. Determine extent of signaling abnormalities and potential mechanism of IFN signaling defect in breast cancer.
- Continue histological analysis of tumor and TDLN tissue sections, and analyze geometrical relationships between cell populations using novel tools and techniques that we developed.
- Utilize biological data generated in this project in the immune regulatory network model that we are developing.

REPORTABLE OUTCOMES: On-going from efforts from this year.

CONCLUSIONS:

In year 2, we made early progress in multiple areas of this project. We have an efficient system in place to recruit patients into this study and procure their samples. However, limited numbers of subjects available and limited amounts of clinical materials available from each subject remain major challenges to the success of this project – we continually attempt to address and solve this issue. We have developed a powerful set of immunological assays and molecular tools to study these samples in greater detail than previously possible. We are constantly striving to minimize the numbers of cells we need to generate useful data, and have to make decisions to pursue only the most promising assays with many samples. This is illustrated by our decision to not pursue the epigenetic studies that we originally proposed, as there are simply too few cells available for this exploratory analysis. We are beginning to uncover dramatic changes in the immune cell populations within tumors, TDLNs, and peripheral blood from breast cancer patients. These will provide important insights into how breast cancer alters the host immune system. We look forward in the coming year to build upon the early data we are generating to come up with meaningful observations and insights into the immunobiology of breast cancer. In the coming year and beyond, we will also begin to make progress on the systems biology that will ultimately position us for the immunotherapy of breast cancer.

REFERENCES:

Rodríguez-Pinto D. B cells as antigen presenting cells. Cell Immunol. 2005;238(2):67-75.
Critchley-Thorne, *et al*. PLoS Medicine 2007; 4:0897
L. Breiman, "Random forests," Machine Learning, vol. 45, no. 1, pp. 5–32, 2001. [Online]. Available: citeseer.ist.psu.edu/breiman01random.html
R. Tibshirani, T. Hastie and J. Friedman, The Elements of Statistical Learning. NY.: Springer, 2001.

Y. Freund and R. Schapire, "A decision-theoretic generalization of on-line learning and an application to boosting," Journal of Computer and System Sciences, vol. 55, no. 1, 1997.
Applied Spatial Statistics for Public Health Data Lance Waller, Carol Gotway, Wiley.
Gomez-Rubio et al. (2005). Cluster Detection with R. Gomez-Rubio, V., Ferrandiz-Ferragud, J. and Lopez-Quilez, A. (2005).
Detecting clusters of disease with R. Journal of Geographical Systems, 7:189-206.
Statistics for Spatial Data, NAC Cressie, Wiley Interscience, 1993

APPENDICES: None at this time.

SUPPORTING DATA: Tables and figures are integrated into the text above.